DEVELOPMENT OF A NOVEL ANTIMICROBIAL FOOD PACKAGING FILM CONTAINING SILVER NANOPARTICLES

A Thesis

Presented to

The Faculty of the Graduate School

at the University of Missouri

In Partial Fulfillment

of the Requirements for the Degree

Master of Science

By

WEI WANG

Dr. Azlin Mustapha, Thesis Supervisor

JULY 2018

The undersigned, appointed by the dean of the Graduate School, have examined the thesis entitled

DEVELOPMENT OF A NOVEL ANTIMICROBIAL FOOD PACKAGING FILM CONTAINING SILVER NANOPARTICLES

presented by WEI WANG
a candidate for the degree of Master of Science
and hereby certify that, in their opinion, it is worthy of acceptance.

Dr. Azlin Mustapha, Food Science Program

Dr. Mengshi Lin, Food Science Program

Dr. Fu-Hung Hsieh Department of Biological Engineering

ACKNOWLEDGEMENTS

First of all, I would like to thank my academic advisor, Dr. Azlin Mustapha, for providing me the opportunity of studying in the University of Missouri and finishing my Master's degree. She is always patient with my mistakes and generous in giving advice when I faced difficulties in research and life. I appreciate all of her helps and guidance. It is my honor to have her as my advisor.

Thank my committee members, Dr. Mengshi Lin and Dr. Fu-Hung Hsieh, for their professional advice and valuable comments. They are kind and patient. I would not have finished this work without their assistance. Thank Dr. Ingolf Gruen, Dr. Bongkosh Vardhanabhuti and Dr. Andrew Clarke for teaching me a great deal about food science. They enriched my knowledge in the area of sensory, dairy and meat.

I would also like to thank my lab mates, Yuejiao Liu, Chenggeer, Zhilong Yu, Kaiwen Choo, Fouad, Rajiv Dhital and my friends Akkasubha Kotchabhakdi, Minhua Zhu for their accompanies in my life and helps on my study. Thank Muli Shi and Xiaoyu Liu for the wonderful time we have spent in the past three years.

Finally, I want to express my profound gratitude to my parents, the two people in the world I love most, for their unfailing love, trust, encouragement and support. They always respect my choice and give me enough space to develop myself. Also, thank my grandparents who always think for me and take care of me, and my cousins who support me all the time.

TABLE OF CONTENTS

LIST OF TABLES

LIST OF FIGURES

DEVELOPMENT OF A NOVEL ANTIMICROBIAL FOOD PACKAGING FILM CONTAINING SILVER NANOPARTICLES

Wei Wang

Dr. Azlin Mustapha, Thesis Supervisor

ABSTRACT

In this study, silver nanoparticles (AgNPs) were incorporated into bacterial nanocellulose (BNC) by a reduction (R) and UV-assisted (UV) methods with the addition of polyvinyl alcohol (PVA) to prepare an environmentally friendly antimicrobial AgNP/PVA/BNC film. The flexibility of BNC was greatly improved by mixing with 3% PVA solution. The films exhibited good mechanical property and higher oxygen barrier capacity. The results of scanning electron microscopy (SEM) showed the surface structure of the films and the uniform incorporation of AgNPs. Antimicrobial activities against *Escherichia coli* O157:H7 were observed from both R and UV films. The UV film showed a higher antimicrobial activity than the R film in all the antibacterial experiments. Up to 7 and 3 log CFU/mL of reductions were observed in liquid medium and on raw beef, respectively. Moreover, a beef shelf-life test suggested that the films were able to inhibit the growth of bacteria on raw beef for at least 10 days at 4 ^{o}C. The physical and antimicrobial properties described above give the AgNP/PVA/BNC films a potential in application of food packaging.

CHAPTER 1 INTRODUCTION

Food packaging plays an important role in food quality because it protects food from physical and chemical damages. To improve the functional properties of food packaging materials, new structural materials and antimicrobial ingredients have been studied. Nanomaterials, such as nanocellulose and nanoparticles, are currently accepted in the food industry due to their unique properties (Laux and others 2017). Bacterial nanocellulose (BNC) is an unbranched polymer with nanofibrils, made up of β-1,4 glycosidic linked glucose units. Its outstanding physical and chemical properties, including high water absorbency, high degree of crystallinity, large surface area, excellent mechanical strength and permeability, make BNC a promising material for development of an effective food packaging material. BNC has been explored for its use in the food industry as a dietary aid, in cosmetics as mask materials, and in the pharmaceutical industry to control drug delivery (Ullah and others 2016). Moreover, the active functional hydroxyl groups of BNC make it suitable for surface modifications. BNC covered with calcium-deficient hydroxyapatite was used in bone tissue engineering (Grande and others 2009). BNC modified with TEMPO was reported to increase water retention (Spaic and others 2014). BNC also acts as a reducing agent in synthesizing nanoparticles and stabilizers when mixed with other materials (Yang and others 2012b).

Antimicrobial activity has been conferred in BNC using metallic nanoparticles, such as zinc oxide quantum dots (ZnO QDs) (Jin and others 2009) and copper

nanoparticles (CuNPs) (Abou-Yousef and others 2018). Silver nanoparticles (AgNPs) are tiny metallic material (diameter of 20 – 100 nm) with a high surface area. AgNP-modified products have been applied in wound healing (Maneerung and others 2008) and for inhibiting foodborne bacteria (Pandit and others 2017) due to its outstanding antimicrobial ability. The most commonly used method of synthesizing AgNPs is via chemical reduction by reducing agents, such as hydrazine hydrate, sodium borohydride ($NaBH_4$) or N,N-dimethylformamide (Peng and others 2017). Other methods, like plant extract reduction (Ribeiro and others 2018) and ultraviolet (UV) reduction (Tao and others 2016), have been conducted as green synthesis.

In previous studies, AgNPs have been successfully incorporated in BNC, and the antimicrobial activity of the AgNP-modified BNC film was evaluated by agar diffusion tests (Berndt and others 2013). Polyvinyl alcohol (PVA) has been mixed with AgNPs and microcrystalline cellulose to make a PVA/NC/Ag nanocomposite film (Sarwar and others 2018). However, the antimicrobial activity of AgNP-modified BNC film on a food sample has never been studied.

The purpose of this study was to develop a flexible antimicrobial food packaging film using BNC, PVA and AgNPs. AgNPs were synthesized by both the reduction and UV methods. Physical properties of the films, including color, micro-structure, mechanical property, water vapor permeability and oxygen barrier capacity were fully characterized by the appropriate instrumentation. Antimicrobial activities of films were evaluated both in vitro and on beef samples. The differences between the films made from the reduction and UV methods were analyzed.

CHAPTER 2 LITERATURE REVIEW

2.1 Cellulose

Cellulose is a highly crystalline linear polymer of glucose. It is an unbranched polymer with nanofibrils, made up of β-1,4 glycosidic linked glucose units (Rajwade and others 2015). Cellulose has become more and more popular because of its outstanding physical and chemical properties, including high water absorbency, high degree of crystallinity, large surface area, excellent mechanical strength, and permeability. The sources of cellulose include plants, animals and bacteria where it exists extensively as a structural element in their cells and is produced every day. In plants, cellulose always combines with lignin, hemicelluloses and other materials which provide protection against outer forces (Turner and Kumar 2018). Cellulose was also extracted from animals, such as tunicates and chicken feathers, but it is not yet in large-scale commercial applications.

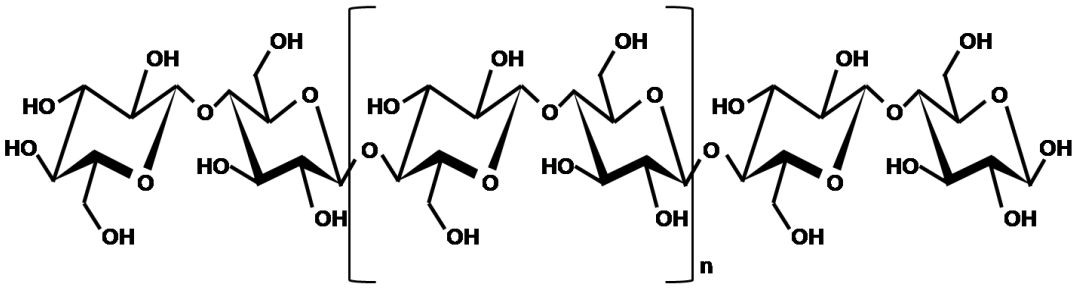

Figure 1 Chemical structure of bacterial nanocellulose (George and Sabapathi 2015).

2.1.1 Physical and chemical properties of bacterial nanocellulose

Bacterial nanocellulose (BNC) was first mentioned in 1886 by Brown (1886). Compared with plant cellulose, BNC is in a much purer form. Because no lignin, pectin or hemicelluloses is mixed in, it is easier to be refined (Chawla and others 2009). BNC has a three dimensional network structure that consists of nano-sized fibers, and hence exhibits great mechanical properties. As reported by Yamanaka and others (1989), air-dried BNC synthesized by *Acetobacter aceti* AJ12368 had a high Young's modulus of >18 GPa and a tensile strength of 260 MPa. The Young's modulus of single BNC nanofibers was reported to be 78 ± 17 GPa (Guhados and others 2005). Compared with other types of cellulose, BNC is well-dispersed and easier to be hydrated in aqueous medium. It is able to emulsify kerosene (Ougiya and others 1997), soybean oil (Blaker and others 2009), olive oil (Owen and others 2000) and liquid paraffin (Jia and others 2016) to obtain stable Pickering emulsions. The emulsification of BNC is considered to be environmentally friendly, edible, nontoxic and biocompatible. Moreover, BNC hydrogel has a very high water-holding capacity (100 times its own weight) and good permeability to liquid and gases due to its porous structure.

The chemical property of BNC is another hot topic. The active functional hydroxyl groups of BNC make it suitable for surface modifications. BNC covered with calcium-deficient hydroxyapatite was used in bone tissue engineering (Grande and others 2009). BNC modified with chitosan showed great improvements in physico-mechanical and biomedical properties (Ha and others 2011). BNC modified

with TEMPO was reported to increase water retention (Spaic and others 2014). BNC also acts as a reducing agent in synthesizing nanoparticles and stabilizers when incorporated with other materials.

2.1.2 Bacterial nanocellulose synthesis

BNC is produced by some bacteria belonging to the genera *Acetobacter, Rhizobium, Azotobacter, Salmonella, Escherichia,* and *Sarcina* (Shoda and Sugano 2005). The type of cellulose-synthesizing organism determines the size and degree of crystallization of BNC fibers. When inoculated in an appropriate medium, these bacteria are able to produce cellulose nanofiber that will subsequently assemble to form a cellulose network. The nanofiber with a diameter of approximately 1.5 nm consisted of 10–15 of cellulose chains which are produced externally through pores in the bacterial cell walls (Brown 1886).

The growth medium plays an important role in the synthesis of BNC. The most commonly used medium is Hestrin and Schramm (HS) medium (Hestrin and Schramm 1954) and corn steep liquor and fructose (CSL-Fru) medium (Bae and others 2004). The main ingredients in these media are glucose which acts as an energy source and cellulose precursor, yeast extract and peptone which provides nitrogen.

2.1.3 Bacterial nanocellulose applications

On account of the fact that BNC has a higher purity, tensile strength and crystallinity, lower density and greater biocompatibility than other celluloses, it is widely used in a variety of contexts. The usage of BNC in the food industry was

approved by the US Food and Drug Administration (FDA) in 1992. BNC as a thickening and stabilizing agent is added in high water content food for gelling and water binding (Shi and others 2014). BNC as a fat-replacement was used to make dietary foods, such as low-calorie meatballs (Lin and Lin 2004) and pork frankfurter (Yu and Lin 2014). BNC containing nisin as food packaging was reported be able to control *Listeria monocytogenes* on frankfurter sausages. In the medical field, BNC works well in wound treatment (Sulaeva and others 2015). BNC would reduce the wound healing cost by lowering the numbers of wound dressing changes and shorten the wound healing time, especially for chronic and burn wounds (Czaja and others 2007). BNC as a biomaterial was also used in making artificial skin and artificial blood vessels (Shah and others 2013). Moreover, the use of fragmented BNC in improving paper flexibility and durability has been reported (Ashjaran and others 2013).

The addition of BNC would help to decrease costs and develop an environmentally friendly industry. Other potential applications of BNC like drug delivery and waste purification were also studied, but further efforts are necessary (Jozala and others 2016).

2.2 Nanoparticles

Nanoparticles (NPs) are manufactured materials that have one or more external dimensions of less than 100 nm. They are individual particles which can be applied to surfaces or integrated into other materials. The concept of NPs was inspired

by Greiling (1954). Later in 1959, a talk by Richard Feynman came up with a thought of controlling matter at the nanoscale, including controlling individual atoms, and that was considered the origin of nanotechnology. In 1960s, the first NPs for drug delivery purposes were developed by Kreuter (2007). In 2001, the National Nanotechnology Initiative was established by President Bill Clinton. The history of NPs until now is over 35 years with a rapid development. Now, studies focusing on NPs are reported every year and their number is increasing exponentially. Researches about NPs are quite popular as they focus on solving big issues that are almost imposable to be solved by regular materials.

2.2.1 Physical and chemical properties of nanoparticles

NPs can be broadly classified into three categories: one dimension nanoparticles, like some thin films or monolayers; two dimension nanoparticles, like carbon nanotubes; and three dimension NPs, such as dendrimers and quantum dots. Unlike the bulk materials, nanoparticles vary in surface morphology, including size, shape and surface charge. It is very important to understand the surface condition of NPs since it influences the physical properties and stability of the nanomaterials. Those features can be evaluated by scanning electron microscopy (SEM), transmission electron microscopy (TEM) and atomic force microscopy (AFM). According to previous studies, the size of NPs varies in materials. Nanocrystal quantum dots are one of the smallest nanoparticles with a diameter of 2–9.5 nm. These NPs exhibit bright fluorescence, narrow emission, broad UV excitation, and are mainly synthesized with II-VI and III-V column elements. Dendrimer, a highly

branched monodisperse polymer system produced by controlled polymerization, has an average particle size less than 10 nm. Polymeric micelles, core/shell structures formed by amphiphilic block copolymers, have diameters of 10 –1000 nm. Metallic NPs, tiny metallic materials with a high surface area, have diameters of 20 – 100 nm. Metallic NPs as the most commonly used nanomaterials are widely applied in drug delivery and highly sensitive diagnostic assays (Nahar and others 2006).

2.2.2 Antimicrobial activity of metal nanoparticles

Metal NPs have been used as effective antibacterial agents because of their outstanding antimicrobial activities. Based on previous studies, the factors that would influence the ability of nanomaterials in inhibiting bacteria can be concluded as follows: NP shape, size, concentration, surface charge, metal ion release, type of surrounding medium, medium pH, presence of oxygen, bacterial cell wall structure and shape and contact area between the nanoparticles and the microbial cell.

When it comes to the antimicrobial activity, AgNP has been shown to be most effective. In the past decade, AgNPs have been reported to successfully inhibit the growth of *Escherichia coli* (Sondi and Salopek-Sondi 2004). A study from Seong reported an antimicrobial activity of AgNPs against *Salmonella* Typhimurium, and stated that the activity is controlled by an inner membrane dysfunction involving reactive oxygen species (ROS)-independent Ca^{2+} imbalance (Seong and Lee 2017). *L. monocytogenes* was reported to be more sensitive than *Staphylococcus aureus* to a green synthesized AgNPs (Awwad and others 2012). The mechanism of antimicrobial activities is not clear, but many potential theories have been reported. A cell

membrane dissolution theory states that silver ions released from silver NPs (AgNPs) would dissolve cell membranes and affect transcriptional responses (McQuillan and others 2012). The DNA damage theory claims that the NPs would adhere to the surface of bacterial cells, alter their membrane properties and damage the DNA, followed by affecting the protein functions (Reidy and others 2013). Another study showed that AgNPs may interrupt the energy source and cause the death of cell (Cao and others 2011).

Gold NPs (AuNPs) showed high activity against gram-negative bacteria than gram-positive bacteria. AuNPs primarily attach to the thiol functional groups of enzymes (NADH dehydrogenases), they generate high amount of free radicals which interrupt the cell respiratory system (Cui and others 2012). Compared to gram-negative bacteria, Gram-positive bacteria has stronger cell wall structure (Chen and others 2015) which limits the uptake of nanoparticles.

Zinc oxide NPs (ZnONPs) are also identified as an effective antibacterial material. The inhibition of bacterial growth is achieved by the permeation of ZnONPs into the cell membrane and the damages caused by oxidative stress on lipids, proteins and DNA (Kelly and others 1998). Recently, the antibacterial activity of ZnONPs against *S. aureus, S.* Typhimurium and *E. coli* was investigated. It was reported that the growth-inhibiting dose of ZnONPs was 15 μg/mL for *E. coli*, and 5 μg/mL for *Klebsiella pneumoniae* (Brayner and others 2006). Other oxide nanoparticles, such as CuO, NiO and Sb_2O_3, have also been reported against *E. coli*, *S. aureus* and *Bacillus subtilis* (Baek and An 2011).

2.2.3 Toxicity of metal nanoparticles

Due to their small size, NPs can affect a cell's biochemical environment and exhibit different levels of toxicities. Smaller NPs have higher toxicities. Studies on toxicity have been conducted over a variety of NPs.

The toxicity of copper NPs is mainly controlled by temperature, NP concentration, bacterial concentration, aeration and pH. The toxicity can be increased by decreasing the condensation. High temperature, high aeration, and low pH will decrease the condensation and provide more available surface area for interacting with bacteria and increasing the solubility of copper ions (Pramanik and others 2012). In addition, essential proteins and DNA of bacteria can be damaged by hydroxyl radicals which are produced by the metallic and ionic forms of copper (Wang and others 2011).

The toxicity of AgNPs depends on the release of silver ions, with liver being the major target organ, followed by spleen, lungs, and kidney (Zhang and others 2016). When used as skin-contact materials, NPs are shown to enter cells and remain on the skin. Samberg and others (2010) studied the cytotoxicity of AgNPs in human epidermal keratinocytes (HEKs) and indicated that the toxicity comes from residual contaminants in the AgNP solutions, and AgNPs themselves may not cause the increase in cell mortality. Toxicities of nanoparticles can be affected by many factors, including environment, particle size, shape, surface coatings, and target cell types. In most conditions, the smaller the size of NPs, the stronger the toxicity and antimicrobial activity they will have. The plate-shaped AgNPs are more toxic against

a fish gill epithelial cell line (RT-W1) and zebrafish embryos compared with other shaped AgNPs because of the presence of surface defects (George and others 2012). Different surface coatings of AgNPs can control the toxicity by blocking ion release and bacterial or cell contact. AgNP coating with a thin SiO_2 layer was reported to minimize the toxicity (Sotiriou and others 2010). Moreover, some studies found that sulfidation can help decrease the toxicity of AgNPs because of the lower solubility of silver sulfide (Levard and others 2013).

AuNPs are considered relatively safer than other metallic NPs because the natural property of gold is inert and nontoxic. AuNPs exhibit their toxicity through a pinocytosis pathway. They enter the cell and attack the lysosomes without entering the nucleus (Shukla and others 2005).

The toxicity of oxide NPs is concentration- and solubility-dependent. CuONPs were considered have the highest toxicity, followed by ZnO, NiO and Sb_2O_3 NPs. These NPs are able to damage bacterial cells by increasing the NP solubility or producing reactive oxygen species (ROS) which can change the microenvironments near the bacteria (Heinlaan and others 2008). The toxicity of ZnONPs is a combined effect of released Zn^{2+} ions and ZnONPs. It has been reported that 6.8 mg/L of Zn^{2+} ions can be released from 125 mg/L ZnONPs suspension, but the toxicity strength mainly depends on the toxic properties of heavy metals instead of released ions (Baek and An 2011). TiO_2NPs showed high toxicity to *Pseudomonas aeruginosa*, *Enterococcus hire* and *Bacteroides fragilis* under UV light. The photocatalysis of TiO_2NPs disrupt cell respiration by increasing peroxidation of the

lipid membrane polyunsaturated phospholipid component (Wan and others 2011).

2.2.4 Metal nanoparticle synthesis

Gold, silver and copper have been commonly used for the synthesis of metallic NPs. They are currently attracting increasing attention in various fields, such as photography, catalysis, biological labeling, wound healing and surface-enhanced Raman scattering (SERS) detection. Therefore, metallic NP synthesis became an area of constant interest. Particle size and properties vary depending on the method of synthesis. Methods used for NP synthesis include physical, chemical and biological methods. They can be divided into top-down and bottom-up methods according to the movement of NPs in the process.

2.2.4.1 Physical method

Evaporation–condensation is a common physical method of NP synthesis. In this technique, a tube furnace is operated at atmospheric pressure. At the furnace, the raw material is placed in a boat centered and vaporized into a carrier gas. No extra material is needed in this method. The problem with this method is that it consumes a great amount of energy and requires a lot of time to achieve thermal stability (Shishkova and Yastrebov 2015). Another method is laser ablation of metallic bulk materials in solution. A rotating metallic rod is immersed in aqueous solutions and irradiated by an unfocused laser beam with a second harmonic laser (Chen and Yeh 2002). The laser ablation method could change the size of the nanoparticles by changing the laser intensity.

2.2.4.2 Chemical method

Chemical methods, including chemical reduction, electrochemical techniques, physicochemical reduction and radiolysis are widely used for metallic NP synthesis. Chemical reduction is the most commonly used method. The conduction of chemical reduction always comes with the use of a variety of organic and inorganic reducing agents, such as sodium borohydride ($NaBH_4$), sodium citrate, Tollen's reagent, ascorbate, elemental hydrogen, polyethylene glycol block copolymers and N,N-dimethyl formamide (DMF). The electrochemical technique is based on the use of a two-electrode setup. The anode and the cathode made from the bulk metal will be transformed into metallic colloidal particles at a constant working voltage (Khaydarov and others 2009). The biggest advantage of these chemical approaches is that they are able to synthesize a large amount of metallic NPs in a pretty short period. However, contamination of chemicals should be contained since they are usually toxic and are not desired in many food and medical products.

2.2.4.3 Green synthesis

In order to overcome the drawbacks of physical and chemical methods, a green synthesis of NPs have been developed. Green synthesis is a bottom-up approach. It is similar to the chemical reduction method where the chemical reducing agent is replaced by the extract of natural products like leaves or fruits. Compared to other methods, green synthesis is environment friendly, cost effective and easily scaled up for large scale syntheses of nanoparticles since there is no need to use high

temperature, pressure, energy and toxic chemicals (Ahmad and others 2003). Green synthesis approaches include the biological method and the polysaccharide method.

In the biological method, bacteria and plant extracts are widely used. Silver ion has been reported to be reduced to AgNPs by the cell metabolism and leached components of a fungus, *Fusarium oxysporum* (Mukherjee and others 2001). The NP products were exceptionally stable due to capping with proteins secreted by the fungus. In other experiments, the leaf extract of *Croton sparsiflorus* and olive were used for the production of AgNPs (20–25 nm, spherical) and proved to possess good antibacterial activity against *S. aureus*, *E. coli* and *B. subtilis* (Kathiravan and others 2015; Khalil and others 2014). The biological method is directly affected by incubation conditions, especially redox conditions (Deplanche and Macaskie 2008) of the parent compound or metal species, that affect the size, shape and dispersity of the NPs formed.

In the polysaccharide method, polysaccharides like starch are usually used as capping agents and β-D-glucose is used as a reducing agent. The process is performed in a gently heated system (Raveendran and others 2003).

Up to now, the methods of synthesizing Ag, Au, Cd and Pd NPs have been studied, but there is still a need to explore the knowledge of the formation of other metal NPs.

2.2.5 Metal nanoparticle applications

Due to their unique properties, NPs have received much attention from scientists and researchers in different areas. The possible applications of these

nanomaterials are currently popular topics.

2.2.5.1 Human health applications

AgNPs have been used most widely in medical science. AgNP-modified products have been approved by a range of accredited bodies, including the US FDA, US EPA, Korea's Testing, SIAA of Japan and Research Institute for Chemical Industry and FITI Testing and Research Institute (Veeraputhiran 2013). The first commercial NP product containing a drug (Abraxane™, human serum albumin NPs containing paclitaxel) appeared on the market at the beginning of 2005 (Hawkins and others 2008). NPs for diagnostic purposes have been marketed now for over 10 years.

AgNPs are effective in healing various wounds, such as burns, chronic ulcers, toxic epidermal necrolysis, and pemphigus. It was incorporated in nanofibers to produce wound dressings. The AgNPs wound dressings significantly promoted the healing process and decreased wound healing time by an average of 3.35 days without any adverse reactions (Huang and others 2007). Chitosan-AgNP and chitin-AgNP wound dressing were also developed as new products with increasing wound healing and antibacterial efficacy.

AgNPs have been shown to display cytotoxic effects in a variety of cells. AgNPs display cytotoxicity to leukemic cells, such as THP-1, Jurkat, and K562 cells. Poly(N-vinyl- 2-pyrrolidone) (PVP)-coated AgNPs could inhibit the viability of acute myeloid leukemia (AML) cells (Guo and others 2013). AgNPs induced MDA-MB-231 breast cancer cells death through ROS generation and DNA fragmentation (Gurunathan and others 2013). The nuclear-targeting

peptide-conjugated AgNPs will cause DNA double-strand breaks and inhibit the HSC-3 cancer cell (Austin and others 2011). AgNPs have also been proven to have a dose-dependent cytotoxicity to lung cancer cells.

Pharmaceutical sciences have applied NPs in the drug release system. Stable colloidal AuNPs were proposed as an appropriate agent for drug delivery to reduce the toxicity and side effects of drugs (Liu and others 2017). They are capable of transferring proteins (Love and others 2015), peptides (Lu and others 2013) and small interfering RNAs (siRNAs) (Liu and others 2015) due to their high loading ability and biocompatibility.

2.2.5.2 Food industry applications

According to previous studies, NPs have been tested to be very efficient in inhibiting the growth of some foodborne bacteria, such as *B. subtilis*, *S. aureus*, *P. aeruginosa*, *Campylobacter jejuni* and *E. coli*. There is a potential application of silver and gold NPs to be incorporated in other supporting matrices, including low density polyethylene (LDPE), polypropylene (PP), and polyurethane (PU) to provide antimicrobial activity and prolong the shelf life of food products. For food preservation, CaO (1%) was reported to safely preserve meat patties since it stops the growth of pathogenic *E. coli* at freezing temperature (Ro and others 2015).

2.2.5.3 Other applications

Magnetic NPs were used to solve environmental problems. For example, ferrites were reported to exhibit excellent adsorptive properties of pollutants, such as

dyes (Wu and others 2004), phosphate (Zhang and others 2009) and arsenite (Zhang and others 2007). Unlike activated carbon which was considered as a good adsorbent material but is difficult to be recovered and reused, the magnetic NPs, with large surface area and small diffusion resistance, can be easily recovered by magnetic separation, and thus is widely used in wastewater treatment.

NPs as additives were introduced to form composite polymer electrolytes (CPE) which greatly improved the performance of rechargeable batteries. The addition of NPs optimized the dielectric, electrolyte, thermal and mechanical properties of polymer electrolyte by generating more free lithium ions (Wang and Alexandridis 2016).

Silver sulfadiazine creams are used to prevent infection at a burn site. A NP-based fluorescence reporting system increased the fluorescence intensity of individual NPs and was developed to achieve rapid bacterial detection at the single-cell level (Zhao and others 2004). Other products that include baby pacifiers, acne creams, and computer's keyboard have successfully applied AgNPs in their products. Even clothing like socks and athletic wear are using AgNPs to protect consumers from emitting body odor.

2.3 Polyvinyl alcohol (PVA)

Polyvinyl alcohol (PVA) is a water soluble biodegradable synthetic polymer that has excellent film-forming properties. It has a relatively simple structure with a pendant hydroxyl group. The world production of PVA is about 65,000 tons per year

(Lin and others 2014). Its number of production is one of the largest in synthetic water-soluble polymers in the world. PVA can be obtained by two steps: (1) polymerization of vinyl acetate to polyvinyl acetate, and (2) hydrolysis of polyvinyl acetate to PVA. The degree of hydrolysis will affect the purity of PVA which further affect the chemical properties, degree of solubility and biodegradability of PVA. PVA cannot be prepared by the polymerization of vinyl alcohol because its monomer, vinyl alcohol, doesn't exist in a stable form and is easy to rearrange to its tautomer (Hassan and Peppas 2000).

2.3.1 Physical and chemical properties of PVA

PVA is odorless, colorless, tasteless and available in white to ivory granule powder form. It is nonhazardous and degradable and therefore considered environmentally friendly. The aqueous solution of PVA is slightly acidic or neutral. It can decompose immediately beyond 200 ^{o}C as it will undergo pyrolysis at an elevated temperature (Ng and others 2014). PVA can be classified into two types: the fully and partially hydrolyzed grades based on the applications. The melting point of PVA is around 180 - 190 ^{o}C for partially hydrolyzed grade and 230 ^{o}C for fully hydrolyzed grade (Bohlmann 2005).

PVA adhesive can be converted to water resistant products by cross-linking its linear chains with boric acid, some salts and other insolubility agents (Feldman 1989). PVA itself has desirable flexibility, tensile strength, hardness and gas and aroma barrier capacity. It will absorb moisture in high humidity conditions and, thus, reduce its tensile strength but increase its flexibility. Excellent oxygen barrier property of

PVA has been reported (Lim and others 2014; Gaume and others 2011). PVA is also well known for its gelation property in various solvents. The property of PVA hydrogels mainly depends on the type of solvents. Hyon and others (1989) found that PVA gels prepared in mixtures of dimethyl sulfoxide (DMSO) and water is transparent when the ratio of DMSO to water is 0.8, and opaque when the ratio is 0.6. The PVA hydrogels are often used in tissue engineering. PVA can be easily mixed with some other polymers, such as keratin (Kalin and others 2015), dextran (Cascone and others 1999) and BNC (Tang and others 2015). PVA can chemically or physically bound to a NP surface (Guo and others 2010). Another characteristic property of PVA is its solubility. The solubility can be easily affected by the molecular weight, degree of crystallization, and degree of hydrolysis (Maria and others 2008). PVA is biocompatible with human tissues since it has a structure that can absorb protein molecules and engage with minimal cell adhesion, and is nontoxic (Yang and others 2004).

2.3.2 PVA applications

Because of the physical and chemical properties of PVA described above, PVA can be used in a huge range of fields. PVA hydrogel is sensitive to physiological environments, is hydrophilic with soft tissue-like water content and adequate flexibility, and can swell and de-swell water in a reversible direction, making it an excellent candidate for biomedical applications (Sood and others 2014). One of the important applications of PVA hydrogel is in wound dressing. PVA was considered the most frequent polymeric membrane candidate for wound dressings and covers

(Kamoun and others 2017). Zhao and others (2003) prepared PVA carboxymethyl chitosan wound dressings using electron beam irradiation. PVA-alginate hydrogel membranes were prepared using ^{60}Co γ-ray irradiation techniques (Nam and others 2004). PVA-dextran xerogel membranes were prepared using freeze-thaw (F-T) crosslinking cycles (Fathi and others 2011). PVA-glucan membranes have been prepared using a physical blending followed by drying at 110 ^{o}C (Huang and Yang 2008). PVA-gelatin membranes containing-glutaminase were prepared using enzymatic crosslinking, followed by F-T crosslinking cycles (Hago and Li 2013). PVA-hyaluronan hydrogel membranes containing ampicillin were prepared using F-T crosslinking cycles (Fahmy and others 2015).

PVA in the food industry is mainly used as an environmentally friendly food packaging material. Chitosan-modified PVA films have been developed to control the growth of food pathogen (Tripathi and others 2009) and to indicate the food temperature as intelligent packaging (Pereira Jr and others 2015).

PVA is also used as a modifier and aggregate surface pre-treatment agent. PVA is added in small amounts to improve the properties of cement mortar and concrete products (Kim and others 1999). Oil palm shell (OPS) aggregates are reported to be treated by PVA before being used in concrete mixing (Mannan and others 2006). PVA is widely used as a building binding agent, such as a thickening agent for latex paint and seals.

2.4 Foodborne disease outbreaks

Foodborne disease is a huge public health burden. From 1999 to 2015, the average number of annual outbreaks in the United States was 1062 (Jones and Yackley 2018). *E. coli* was recorded as one of the main sources of food microbial contamination. It is commonly found in the intestine of warm-blooded organisms. Although *E. coli* strains are typically non-pathogenic and can even benefit the gut fauna, some of them are able to cause infections with the symptoms of nausea, vomiting, stomach cramps, bloody diarrhea and malaise. Among those pathogenic *E. coli*, *E. coli* O157:H7 was recognized as an important and threatening human pathogen since 1993 when four deaths and more than 700 illnesses were reported in a large multistate outbreak (Davis and others 1994).

E. coli O157:H7 is a Gram-negative rod shape bacteria. It is also known as Shiga toxin–producing *E. coli* (STEC). The major source of STEC contamination is beef products, especially raw beef and ground beef. Fecal contamination during processing is unavoidable, and STEC may grow following beef production. According to Darling (ANSAY and others 1999), the pH and water activity of a meat matrix, temperature and exposure time during processing, transportation and storage are the potential factors that contribute to STEC contamination in beef products. In ground beef, a large surface is produced because of the production of tiny meat particles, increasing the chances of being contaminated by dirty or soiled tools and environments. In addition, the large surface area of ground beef provides an aerobic condition that facilitates rapid bacterial growth.

In recent years, *E. coli* O157:H7 is still a big threaten of food safety. In 2017, 413 outbreaks related with *E. coli* O157:H7 was reported by the Centers for Disease Control and Prevention (CDC) (Marder and others 2018). Therefore, more antimicrobial studies are required to protect foods from pathogens. Food packaging as the main protection of food products during transition and storage, deserves to be further studied.

2.5 Food packaging film

Food packaging is a commonly used material in our daily life. It is mainly divided into three types, called primary, secondary and tertiary packaging. Primary packaging is defined as "a sales unit to the final user or consumer at the point of purchase" (HÄNSCH and KINKEL 1995). Secondary packaging is designed to protect both product and primary packaging, for example, cardboard box. Tertiary packaging is usually used in goods transport and removed before selling. A good packaging must act as a protective system to prevent passage of environmental contaminants into foods. Also, the packaging should be nontoxic, flexible, impermeable to microorganisms and strong enough to withstand mechanical forces from the outside. It is reported that 50% of food produced globally are damaged before reaching consumers (Barlow and Morgan 2013). Foods can be physically destroyed or contaminated by microorganisms when exposed to the environment during processing, packaging and shipping. Traditional packaging can prevent damage from the outside but not destruction of food-borne pathogens. Therefore,

antimicrobial packaging has become an emerging need and is expanding with application of nanotechnologies.

2.5.1 Antimicrobial agents in food packaging

Functions of extending shelf-life and maintaining food quality are induced into an antimicrobial packaging when it is incorporated with antimicrobial agents. Compared to direct addition of preservatives into food, the effectiveness of antimicrobial packaging is greater, mainly because of two reasons. Firstly, the attachment of antimicrobial agents with a polymer film base enables a slow release of the antimicrobial agents, resulting in a longer antimicrobial period. Secondly, direct addition of food preservations may lead to preservative invalidation because of the dilution or hydrolysis of food matrixes and components (Appendini and Hotchkiss 2002). Besides, the addition of preservative may reduce food quality and even cause food safety problems.

One of the most popular antimicrobial agents is essential oil. Rosemary essential oil was incorporated into polyamide films (Han and others 2007). Oregano essential oil was reported to control the microorganisms in packed salad (Muriel-Galet and others 2012). Allyl isothiocyanate (AIT) was used to inhibit the growth of *E. coli* O157:H7 in ground beef (Nadarajah and others 2005). Garlic oil was used to protect sprouts (Gamage and others 2009). Other antimicrobial agents, including enzymes (Güçbilmez and others 2007), chitosan (Joerger and others 2009), bacteriocin (An and others 2000) and inorganic NPs were also reported to be used in antimicrobial food packaging.

2.5.2 Nanotechnologies in food packaging

Nanotechnology has the potential to enhance the properties and overcome the drawbacks of traditional packaging materials. It is able to reduce material use, process cost and improve environmental performance. The application of nanotechnology in packaging mainly depends on two methods: disperse nanophases into a polymer matrix and coat nanophases on polymer surfaces.

The nanomaterial incorporation is conducted by mixing nanomaterials with polymers. In this technique, bio-based nanomaterials, nanofibers or nanocrystals which can be derived from plants, bacteria or animals, are commonly used. Because they can improve strength and gas barrier, their application in food packaging has been explored.

Nanocoating has been studied for decades, and some of them are widely used in industry today. The idea of nanocoating is to incorporate the nanomaterial on the surface of a thin layer of material which acts as a barrier. Recent studies have reported enhanced barrier properties in NP-coated polymer materials. Nanoclay-polymer composite, for instance, showed good gas barrier properties, and is widely used in the cheese and processed meat industries (Miller and Senjen 2008). Antimicrobial activity is also induced in packaging by coating metal NPs.

Generally speaking, the application of nanotechnology in food packaging has benefits related to shelf-life extension, higher product quality, improved consumer experience and security. It greatly improved the physical and chemical properties of packaging. The use of nanotechnology will continue to grow in the future. More

studies will be needed to explore the benefits of nanotechnology.

2.5.3 Food packaging materials

In addition to antimicrobial agents, film materials also play an important role in packaging. They act as the base of packaging. Packaging can be divided into two groups: biodegradable packaging and non-biodegradable packaging. Most packaging materials are non-biodegradable. The improper recycling of non-biodegradable packaging has caused environmental pollution worldwide, especially in developing countries, but it is still widely used in packaging manufacture because of the advantages of low density, low cost, high transparency, high mechanical strength, excellent barrier properties and ability to be heat-sealed. Those materials include low density polyethylene (LDPE), linear low density polyethylene (LLDPE), high density polyethylene (HDPE), polyethylene terephthalate (PET), ethylene vinyl acetate (EVA), polypropylene (PP), polystyrene (PS) and polyvinyl chloride (PVC).

In recent years, a shift towards increasing usage of biodegradable packaging has occurred. Usually the biodegradable packaging is produced by blending thermoplastic starches (TPS) with polylactic acid (PLA). PLA is produced by fermentation from renewable resources. It is the most widely used polymer. Other examples of biodegradable polyesters are polyhydroxybutyrate-co-hydroxyvalerate, polycaprolactone (PCL), poly(butylenes adipate-co-terephtalate), poly(hydroxyl ester ether) and polybutylene succinate-adipate. PVA was also mentioned in other studies as a special synthetic polymer with biodegradable characteristic and is generally blended with natural polymers because of its hydrophobic property, nontoxicity and good

water solubility (Sung and others 2013).

2.5.4 Antimicrobial agent coating methods

Some of the antimicrobial agents are sensitive to the conditions used in packaging processes. Their effectiveness might be reduced by high temperature or pressure. As reported by Suppakul and others (2002), in their carvacrol and thymol modified PP film, only 3.5% w/w antimicrobial agents remained after a hot press process (Ramos and others 2012). A greater loss of about 96.7% weight after a blown film extrusion process was reported in a LLDPE-based packaging.

In order to reduce the loss of antimicrobial agents, refined technologies were operated. Surface coating and electrospinning methods were employed for temperature sensitive antimicrobial agents. Elevated temperature processes were reported to have a higher antimicrobial ability than the coating method (Solano and de Rojas Gante 2012). A lower temperature can be approached in cast film. It is limited for natural polymers which have a relatively low melting temperature, such as starch, chitosan, PLA, WPI and PVA. These kinds of films are usually edible and biodegradable depending on the ingredients.

2.6 Objectives of this research

This study is aimed to produce environmentally friendly food packaging films based on AgNP/PVA/BNC with enhanced mechanical and antimicrobial properties. BNC was used as a reinforcing nano-filler and PVA was chosen as the matrix. AgNPs prepared from two methods acted as an antimicrobial agent and conferred the

antimicrobial ability to the film. Physical and chemical properties of the AgNP/PVA/BNC films were evaluated through Fourier transform infrared (FTIR), ultraviolet-visible spectra, scanning electron microscopy (SEM) and inductively coupled plasma mass spectrometry (ICP-MS). The antimicrobial activity of the films against *E. coli* O157:H7 were studied in broth culture and on raw beef.

CHAPTER 3 MATERIALS & METHODS

3.1 Materials and chemicals

Plate count agar (PCA), tryptic soy broth (TSB), tryptic soy agar (TSA), MacConkey sorbitol agar and peptone were purchased from Fisher Scientific (Pittsburgh, PA, USA). Silver nitrate ($AgNO_3$), sodium borohydride ($NaBH_4$), glycerol, and 99% hydrolyzed polyvinyl alcohol (PVA) were purchased from Sigma-Aldrich (St. Louis, MO, USA). Deionized water was prepared by a water purification system (Millipore, Billerica, MA, USA). Top round beef was purchased from Lucky's Market (Columbia, MO, USA).

3.2 Synthesis of BNC slurry

BNC was synthesized by statically cultivating *Gluconobacter xylinus* ATCC 53582 in Hestrin and Schramm (HS) medium at 26 ^{o}C for 7 days. HS medium was made by dissolving 20 g glucose, 5 g peptone, 5 g yeast extract, 2.7 g disodium phosphate, and 1.5 g citric acid in 1 L of deionized water (Gao and others 2016). The resulting BNC was purified by soaking in 500 mL deionized water at 70 ^{o}C for 3 h and 500 mL 0.1 N NaOH solution at 70 ^{o}C for 90 min, followed by washing in deionized water until the pH of the BNC approached 7.0. Around 12 g (wet weight) of BNC was synthesized in each plate. The purified BNC was homogenized at high speed (120 volts, 60 Hz and 3.0 amps) for 30 min using a Waring blender (Model

51BL31, Torrington, CT, USA) to form BNC slurry.

3.3 Incorporation of silver nanoparticles (AgNPs) into BNC slurry by a reduction method

The obtained BNC slurry (5 g) was immersed in 10 mL 0.01 M $AgNO_3$ solution for 1 h at room temperature. The $AgNO_3$/BNC slurry was centrifuged at 5,916 x*g* for 10 min to separate the slurry from the solution. The slurry was then soaked in 10 mL 0.02 M $NaBH_4$ solution for 10 min in an ice bath. The formation of AgNPs was observed as the color of the slurry changed from bright yellow to brownish yellow. A AgNP/BNC slurry was obtained by washing with deionized water and centrifuging at 5,916 x*g* for 10 min to remove unincorporated chemicals.

3.4 Incorporation of AgNPs into BNC slurry by a UV method

The BNC slurry (5 g) was immersed in 10 mL 0.1 M $AgNO_3$ solution and exposed to a 243 nm ultraviolet (UV) light for 1 h at room temperature. During this exposure, the BNC functional groups were activated by UV light and the Ag ions were reduced to Ag NPs (Basuny and others 2015). AgNP/BNC slurry was obtained by centrifuging at 5,916 x*g* for 10 min.

3.5 Preparation of AgNP/PVA/BNC films

Three grams of PVA crystals (Sigma-Aldrich, St. Louis, MO, USA) were dissolved in 100 mL distilled water and autoclaved at 121 ^{o}C for 20 min to form a 3%

PVA solution. Five grams of the AgNP/BNC slurry and 1 g of glycerol were added to the 3% PVA solution and the mixture was stirred for 30 min at 90 ^{o}C. In this step, AgNP/PVA/BNC films made from the reduction method (R film) and AgNP/PVA/BNC films made from the UV method (UV film) were obtained by using AgNP/BNC slurries from the respective methods described above. Finally, the films were formed by casting the solution in 100 × 15 mm sterile plastic petri dishes (USA Scientific, Ocala, FL, USA) and drying at 45 ^{o}C for 12-16 h.

3.6 Color measurement

The color of the films was tested by colorimeter (Chroma Meter CR-410, Konica Minolta Sensing, Inc., Osaka, Japan). Pure BNC film and PVA/BNC film which contained no AgNPs were tested as the control. The R and UV films were tested to indicate the effect of AgNPs on color. A three dimension "Lab" color space was used to describe all perceivable colors. To indicate the difference between the color of the sample and a standard, the total color difference (∆E) was calculated according to the following equation (Paschoalick and others 2003):

$$\Delta E = [(L^* - L_0^*)^2 + (a^* - a_0^*)^2 + (b^* - b_0^*)^2]^{½}$$

where L*, a*, b* correspond to the color parameters of the film sample and L_0*, a_0*, and b_0* correspond to the color parameters of the standard.

3.7 Mechanical properties

The mechanical properties of the films were examined using a texture analyzer (Texture Technologies Corp., Scarsdale, NY, USA) with the aid of a 5 kg load cell at 25 ^{o}C. In order to ensure that the readings truly originated from the middle of the films, films were cut into hourglass-shaped pieces with a middle width of 1 cm, end width of 2 cm and length of 5 cm. The samples were stretched with a force of 50 N and a speed of 5 mm/s. The mechanical test was conducted in triplicate with two replications. Tensile strength and elongation at break were calculated by the following equations:

$$\text{Tensile strength (Pa)} = F_{max} / A$$

$$\text{Elongation at break (\%)} = \Delta H / H_0 \times 100$$

where F_{max} is the maximum force (N), A is the cross-sectional area (thickness $\times$ width) of the film sample (m^2), ΔH is the increased height of the edible film (mm), and H_0 is the initial distance between grips (mm).

3.8 Fourier transform infrared (FTIR) spectra

The existence of specific chemical groups of the AgNP/PVA/BNC films was confirmed by a Nicolet 380 FT-IR spectroscopy (Thermo Electron Corp., Madison, Wisconsin, USA). Films were directly measured using an attenuated total reflectance (ATR) accessory. Spectra were obtained by the accumulation of 64 scans at 4000-400

cm^{-1} wavenumber with a resolution of 4 cm^{-1}.

3.9 Ultraviolet-visible spectra

The formation of AgNPs was characterized by UV–visible spectroscopy (Cary 50 spectrophotometers, Varian, Mulgrave, Victoria, Australia). To get a comparative absorption spectrum, AgNP/BNC slurry made from the R and UV methods were prepared in solutions (100 mg/mL). A solution of pure BNC slurry was prepared as a control. The solutions were centrifuged at 5,916 x*g* for 10 min, and the supernatant was scanned in the wavelength range of 200–800 nm.

3.10 Scanning electron microscopy (SEM) and energy dispersive X-ray spectroscopy (EDS)

The structure of the AgNP/PVA/BNC film and the presence of AgNPs were examined by a scanning electron microscope (SEM) (Quanta 600 FEG; FEI Company, USA) equipped with energy dispersive X-ray spectroscopy (EDS) capability. Film samples were sputtered with platinum. Images were collected at 10 mm working distance with an aperture size of 6 and a spot size of 3. EDS analysis was conducted to confirm the presence of Ag ions.

3.11 Transmission electron microscopy (TEM)

In order to study the antimicrobial mechanism of AgNP/PVA/BNC films, R and UV films were cut into 1.5 cm × 3 cm pieces and placed in 10 mL of fresh *E. coli*

O157:H7 (10^6 CFU/mL) cultures, respectively. The cultures were incubated at 37 ^oC for 24 h, followed by centrifuging at 13000 x*g* for 5 min to obtain concentrated samples. Samples were dried on a carbon-coated copper grid and observed by a transmission electron microscope (TEM) (Hitachi, H7650) at 100 kV.

3.12 Membrane permeability test

One gram of AgNP/BNC slurry made from R and UV methods were added into respective test tubes containing 10 mL of fresh *E. coli* O157:H7 culture. Cultures treated with no slurry and pure BNC slurry were set as controls. Cultures were incubated at 37 ^oC for 10 h, and 1 mL of each treated culture was centrifuged at 13,000 x*g* for 5 min and resuspended in peptone water. The suspensions were examined by UV spectroscopy (Cary 50 spectrophotometers, Varian, Mulgrave, Victoria, Australia) at the wavelength of 260 nm for DNA absorbance and 280 nm for protein absorbance.

3.13 Water vapor transmission rate (WVTR)

The water vapor transmission rate (WVTR) was evaluated by following a modified ASTM E96-90 (ASTM, 2002) method. Glass jars (outer diameter of 2.6 cm, inner diameter of 1.4 cm, 5.9 cm deep) containing 10 mL distilled water were covered with PVA/BNC, R and UV film samples and sealed with masking tape (ShurTech Brands, LLC Avon, OH). The jars were placed in a desiccator with fresh desiccant, whose relative humidity was kept at 50%, and stored at 25 ^oC for 24 h. The weight of

the jars was measured at 0 and 24 h. WVTR was calculated using following formula:

$$\text{WVTR } (g/m^2 \text{ day}) = (\Delta w/\Delta t)/A$$

Where Δw is the weight change, Δt is the time period, and A is the film area exposed to the moisture transfer.

3.14 Oxygen barrier

The oxygen barrier property of AgNP/PVA/BNC film was measured according to a method using corn oil (Du and others 2016). Fresh corn oil was poured into 50 mL glass jars (25 mL in each). Jars were then covered with PVA, PVA/BNC, R or UV films and stored at 65 ^{o}C for 7 days. An open jar was set as the control. After storage, the peroxide value (POV) of the corn oil was measured by a sodium thiosulfate titration method which was described previously (Jin and others 2010). POV was calculated by the following equation: POV (meq/kg) = $1000 \times (V_1 - V_2) \times (N/M)$, where V_1 and V_2 are the volume of sodium thiosulfate solution used for the sample and blank determination (mL), N is the concentration of sodium thiosulfate solution (M), and M is the weight of the oil sample (g).

3.15 Release test

To quantitatively analyze the silver release of AgNP/PVA/BNC films *in vitro*, the R and UV films were cut into squares with side lengths of 4.0 cm, and

individually immersed in 15 mL of physiological saline solution (0.9% sodium chloride solution) at 37 ^{o}C. Two milliliters of immersion solution were removed at regular time intervals (0, 12, 24, 72 and 168 h). The silver ion content was analyzed by inductively coupled plasma mass spectrometry (ICP-MS) (Leeman, USA). The release ratio of silver was calculated using the silver content in the immersion solution divided by the original silver content in the composites.

3.16 Antimicrobial activity of the AgNP/PVA/BNC films

3.16.1 Bacterial inhibition test

Escherichia coli O157:H7, consisting of *E. coli* O157:H7 C7927, *E. coli* O157:H7 EDL-933, *E. coli* O157:H7 MF-1847, *E. coli* O157:H7 505B and *E. coli* O157:H7 3178-85 were separately cultivated in 10 mL of TSB for 24 h at 37^{o}C. The concentration of each strain was determined by the pour-plating method using TSA. Different volumes of each strain was used to obtain a five-strain *E. coli* cocktail with the bacterial strain ratio of 1:1:1:1:1. The cocktail was then diluted in peptone water to obtain a concentration of approximately 1×10^4 CFU/mL and divided into sterile test tubes with 10 mL in each tube. The R and UV films were cut into 1.5 cm × 3 cm pieces and placed in the test tubes (one piece in each tube). The bacterial culture with no film was set as the control. Samples were incubated in a shaker incubator (Eppendorf, New Brunswick, Hauppauge, New York, U.S.A) with shaking at 120 rpm and 37 ^{o}C. The antimicrobial activity of the AgNP/PVA/BNC film was evaluated by doing a plate count of each sample at 0 h, 3 h, 6 h, 9 h and 24 h.

3.16.2 Beef shelf-life test

A beef shelf-life test was conducted to investigate the antimicrobial activity of the AgNP/BNC/PVA film against natural bacteria on raw beef. For this purpose, the R and UV films in duplicates were set as the treatments. Fresh raw top round beef was aseptically cut into 2 x 2 x 2 cm^3 cubes and wrapped with the films. Unwrapped beef and beef wrapped with PVA/BNC film were included as two controls. Samples were stored at 4 ^oC and removed for plating on TSA at 0, 4, 7, 10 and 14 days. Agar plates were incubated at 37 ^oC for 24 h followed by enumeration of colonies.

3.16.3 Beef inoculation test

Two film treatments (R film and UV film) and two controls (unwrapped inoculated beef and inoculated beef wrapped with PVA/BNC film) in duplicates were set in order to investigate the antimicrobial activity of AgNP/PVA/BNC films against *E. coli* O157:H7 strains on raw beef. One hundred and fifty milliliters of *E. coli* O157:H7 cocktail (1×10^9 CFU/mL) was cultivated in TSB in a beaker for 24 h before the experiment. Raw top round beef was cut into $2.5 \times 2.5 \times 1.25$ cm^3 pieces under aseptic conditions and submerged in the *E. coli* cocktail for 2 min. The inoculated beef pieces were then aseptically transferred onto a sterile steel wire net basket and hung 20 cm above a sterile tray to drip-dry at room temperature in a laminar flow hood for 15 min. After drying, the inoculated beef pieces were wrapped with the different film treatments and stored at 4 ^oC. To evaluate the antimicrobial activity of the films against the pathogens, beef pieces were stomached and plated on

MacConkey sorbitol agar at 0, 4, 7, 10 and 14 days. Agar plates were incubated at 37 ^{o}C for 24 h followed by enumeration of white colonies.

3.17 Toxicity

3.17.1 Toxicity against intestinal bacteria

Lactobacillus paracasei 25598acillus, *Lactobacillus rhamnosus* GG, *Lactobacillus acidophilus* ADH, *Lactobacillus acidophilus* NCFM and *Bifidobacterium animalis* spp lactis Bif-6 were inoculated in MRS broth, and *E. coli* 23716 was inoculated in TSB broth. Bacteria were grown at 37 ^{o}C for 24 h to reach the logarithmic phase. The AgNP/MRS agar and AgNP/TSA agar were prepared by thoroughly mixing 5 g of AgNP/BC slurry with 100 mL melted MRS and TAS agar, respectively. The bacteria were diluted to different concentration (10^1 to 10^9 CFU/mL) using peptone water. A plate count method was conducted for each bacteria using the AgNP/MRS agar, and for E.coli using AgNP/TSA agar. Plate count method using MRS and TSA agar were set as controls. Plates are inoculated at 37 ^{o}C for 24 h. Data was collected by counting the number of colonies grow on the plates.

3.17.2 Toxicity against FHC and Caco-2 cells

3.17.2.1 Cell culture and AgNP/BNC treatments

Fetal human cells (FHC) (ATCC® CRL1831™) were cultured in Dulbecco's Modified Eagle Medium (DMEM) (ATCC 302006), and Caco2 (ATCC® HTB37™) cells were cultured in Minimum Essential Medium (MEM) (ATCC 302003). Cells

were incubated in 75 cm^2 flasks (BD Falcon, Massachusetts, USA) in a 5% CO_2 incubator (New Brunswick, Germany) at 37 ^oC until covering about 80% of flasks. The freshly inoculated cells were dissociated from the flasks and seeded in 96-well plates with a concentration of 100 cells/well. After a 24-hour seeding, the culture medium was replaced by 100 μL new-made medium, and 50 μL of the AgNP/BNC slurry prepared from R and UV methods of different dilutions was add into each well. The plates were incubated in the CO_2 incubator at 37 ^oC for 24 h.

3.17.2.2 MTT assay

The toxicity of AgNP/BNC slurry to FHC and Caco-2 cells was determined by methylthiazolyldiphenyl - tetrazolium bromide (MTT) (3-(4,5-dimethylthiazol-2-yl)-2,5-diphenyltetrazolium bromide) assay. The previous medium was replaced by 100 μL fresh medium containing 10 μL of MTT reagent. After incubating for 2 to 4 h, 100 μL of detergent reagent (MTT kit) was added into each well, followed by a 2-h incubation for color development. Plates were read by a plate reader at the absorbance wavelength of 570 nm. The background was measured at a wavelength of 655 nm.

3.17.2.3 WST-8 assay

A water - soluble tetrazolium salt (WST-8) assays was conducted to confirm the toxicity of AgNP/BNC slurry. A WST-8 mixture was prepared by combining equal volumes of Electron Mediator Solution and WST-8 Developer Reagent. The previous medium was replaced by 100 μL of fresh medium containing 10 μL of WST-8 mixture. The plates were incubated in the CO_2 incubator at 37 ^oC for 4 h and read by the plate

reader at the absorbance wavelength of 450 nm.

3.18 Statistical analysis

All the experiments were performed in triplicate with two replications. Data were expressed as means ± standard deviation (SD), and analyzed by one-way analysis of variance (ANOVA) with a significance level of 0.05.

CHAPTER 4 RESULTS

4.1 Color

The color parameters of the different films are shown in Table 1. The color of pure BNC film is close to the color of the background, a white backing plate. The addition of AgNPs made the film darker, redder and yellower according to the *L*, *a* and *b* value, respectively, resulting in an increase in total color difference ($\triangle E$). This indicated that the color of the AgNP/PVA/BNC films made from both methods were significantly different ($P \leq 0.05$) from the color of pure BNC film. No obvious difference in color was observed between the R and UV films.

Table 1 Color of the films.

Film Sample	***L****	***a****	***b****	∆E
BNC film	97.37 ± 0.03[a]	-0.335 ± 0.01[a]	4.15 ± 0.05[a]	2.25 ± 0.01[a]
PVA/BNC film	98.67 ± 0.05[a]	-0.23 ± 0.02[a]	2.68 ± 0.01[a]	1.03 ± 0.02[a]
R film	65.87 ± 0.71[b]	9.48 ± 0.25[b]	33.89 ± 0.08[b]	46.23 ± 0.6[b]
UV film	68.05 ± 0.41[b]	9.82 ± 0.02[b]	35.14 ± 0.49[b]	45.59 ± 0.04[b]

4.2 Mechanical properties

As compared with pure BNC, the AgNP/PVA/BNC films have lower tensile strength and higher elongation at break, which means that the addition of PVA helped the film became more stretchable (Table 2). The difference in mechanical properties

between the R film and UV film was not obvious, which indicated that the improvement in mechanical properties was mainly achieved by PVA addition. The amount of AgNPs and the method of AgNPs synthesis did not affect the mechanical properties.

Table 2 Film mechanical properties.

Film Sample	BNC	R film	UV film
Tensile strength (MPa)	5.33 ± 0.08^{a}	2.31 ± 0.32^{b}	2.42 ± 0.41^{b}
Elongation at break (%)	12.31 ± 1.02^{a}	295.64 ± 2.63^{b}	241.78 ± 3.34^{b}

4.3 Fourier transform infrared (FTIR) spectra

Fig. 2 shows the FT-IR spectra of the PVA/BNC film and the AgNP/PVA/BNC films. In the BNC spectra, the strongest absorption around 3300 cm^{-1} corresponds to the vibration of intra-chain and inter-chain hydrogen-bonded hydroxyl groups (-OH). Absorption around 2895 cm^{-1} was caused by valence vibration of C-H bond (Pereira and others 2014).

In the PVA/BNC spectra, the peak at 3300 cm^{-1} became smoother, and the peak at 2900 cm^{-1} split into two (2908 and 2938 cm^{-1}) which correspond to the vibration of C-H bond and hydroxyl groups. The absorption around 847 cm^{-1} corresponds to the vibration of the β-1,4-glycosidic linkage. In the fingerprint region of 1500–1000 cm^{-1}, the peaks at 1417, 1326, and 1085 cm^{-1} correspond to the CH_2CH_2 structure, alkoxy

C–O bond, and acyl C-O bond stretching vibrations, respectively (Alila and others 2009). All the absorptions described above are related to the structure of BNC.

In the spectra of the R and UV film, the typical peaks for BNC were found at 3,270, 2,938, 1,417, 1,033 cm^{-1}. No additional absorption was found, except the peak at 1085 cm^{-1} was split into two peaks.

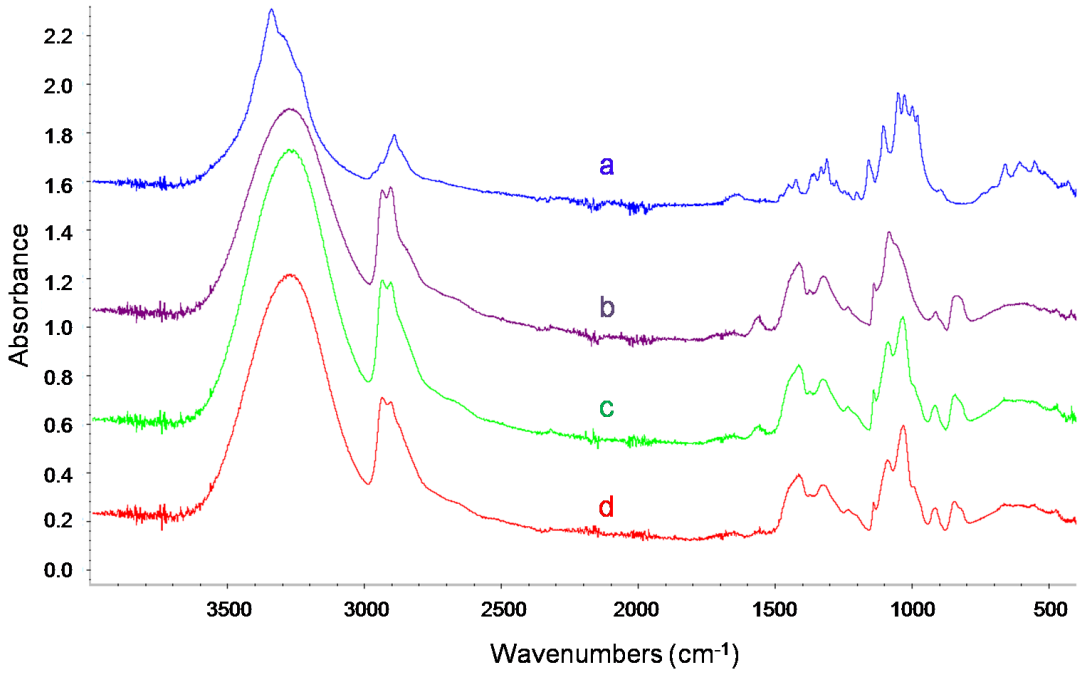

Figure 2 FTIR spectra of pure BNC film (a), PVA/BNC film (b), R film (c) and UV film (d).

4.4 UV-vis spectra

AgNPs as metal nanoparticles have a surface plasmon resonance (SPR) absorption band which is available in the UV–visible region. Therefore, the size and distribution of AgNPs can be easily estimated by measuring the UV–vis absorption spectra of the samples (Li and others 2015). In this study, samples were prepared from the AgNPs/BNC slurry supernatant which contains only a small part of AgNPs of the film, so instead of measuring quantity, the UV-vis spectra was only used to examine

the size and confirm the presence of AgNPs. According to the results shown in Fig. 3a, BNC as a control had no absorption band in the UV–vis spectrum range of AgNPs (390 nm – 460 nm). The AgNP/BNC slurry made from the reduction method exhibit an absorption band at around 405 nm, which indicates a small size of nanoparticles (Fig. 3b) (Stamplecoskie and others 2011). No absorption band was obtained in the AgNP/BNC slurry made from the UV method (Fig. 3c).

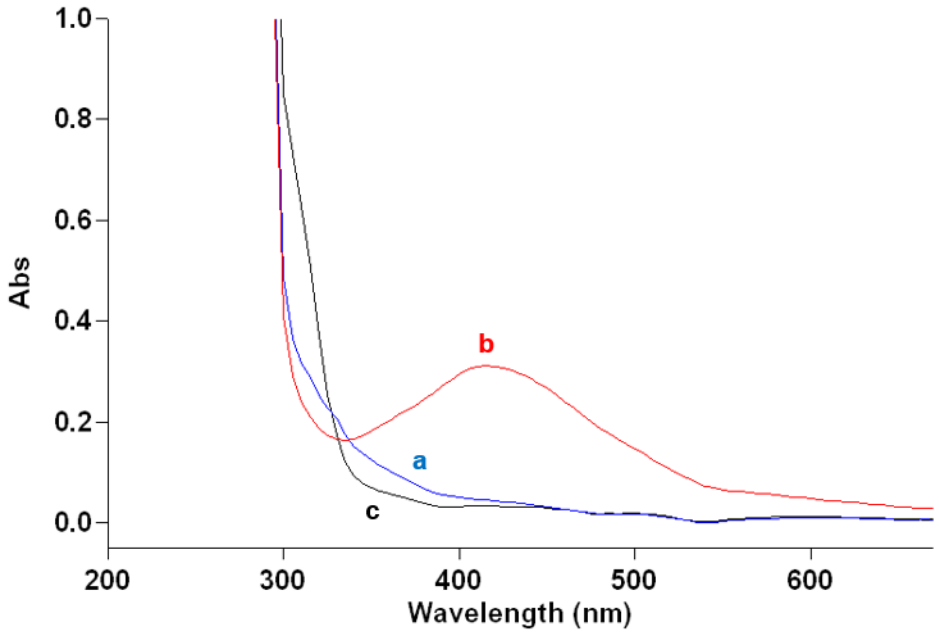

Figure 3 UV–Vis spectra of BNC (a), AgNP/BNC slurry from reduction method (b), and AgNP/BNC slurry from UV method (c).

4.5 Scanning electron microscopy (SEM) and energy dispersive X-ray spectroscopy (EDS)

SEM was used to investigate the surface morphology of AgNP/PVA/BNC films. BNC slurry and PVA/BNC film, as controls, were prepared by air-drying the BNC slurry and PVA/BNC mixture, respectively. As shown in Fig. 4a, nanofibers with the size of around 100 nm in the BNC slurry closely linked with one another,

forming a three-dimensional network. After being modified with PVA, the PVA/BNC film displayed a flat dense surface with nanofibers mixed in (Fig. 4b). For the R and UV films, tiny white spots which are considered as AgNPs can be observed. Spherical AgNPs with a size around 20-30 nm were uniformly dispersed in the film in high density (Fig. 4c and d). The presence of Ag in these two films was confirmed by EDS analysis. Ag elements were identified on both R and UV films (Fig. 5a and b).

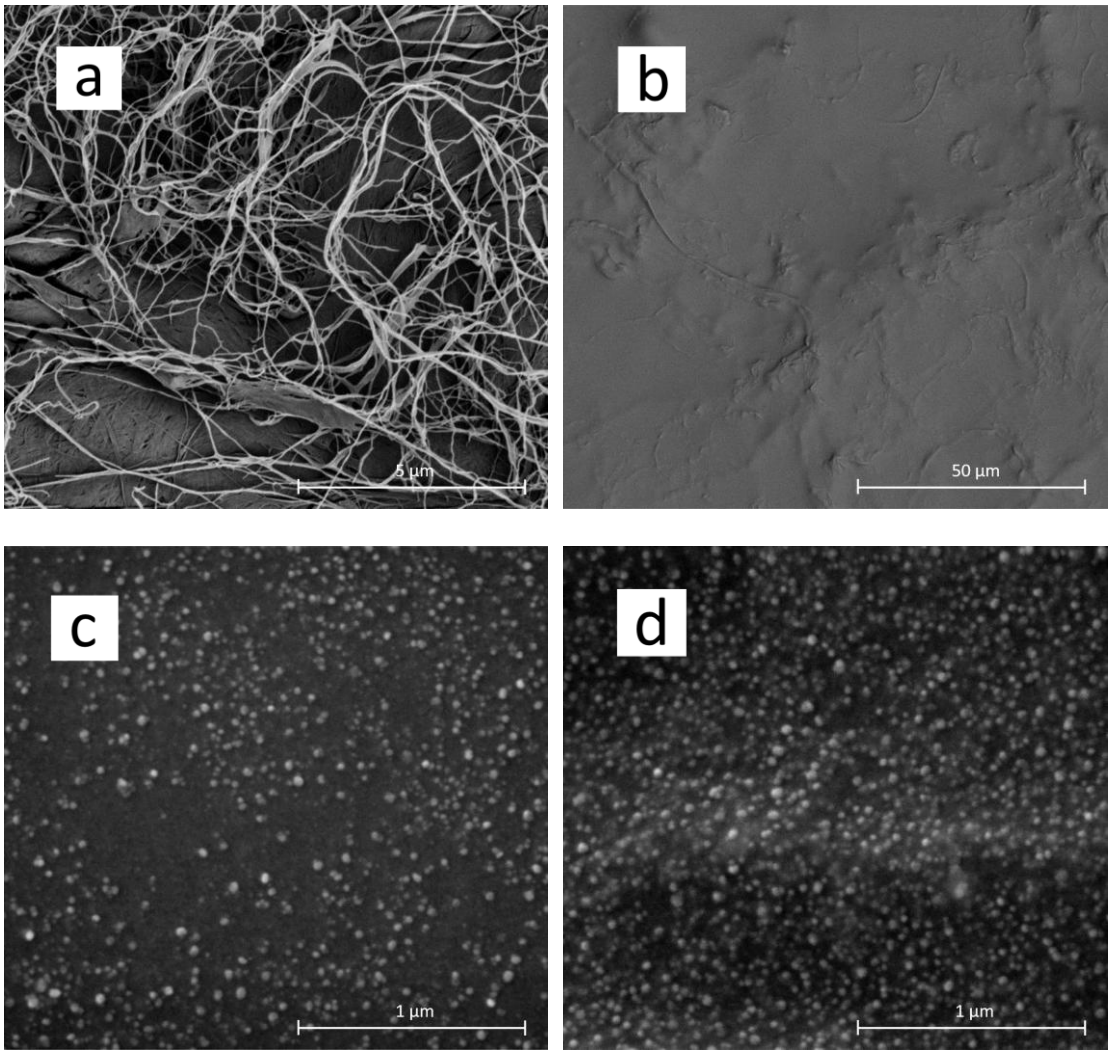

Figure 4 SEM images of (a) BNC slurry, (b) PVA/BNC film, (c) R film and (d) UV film.

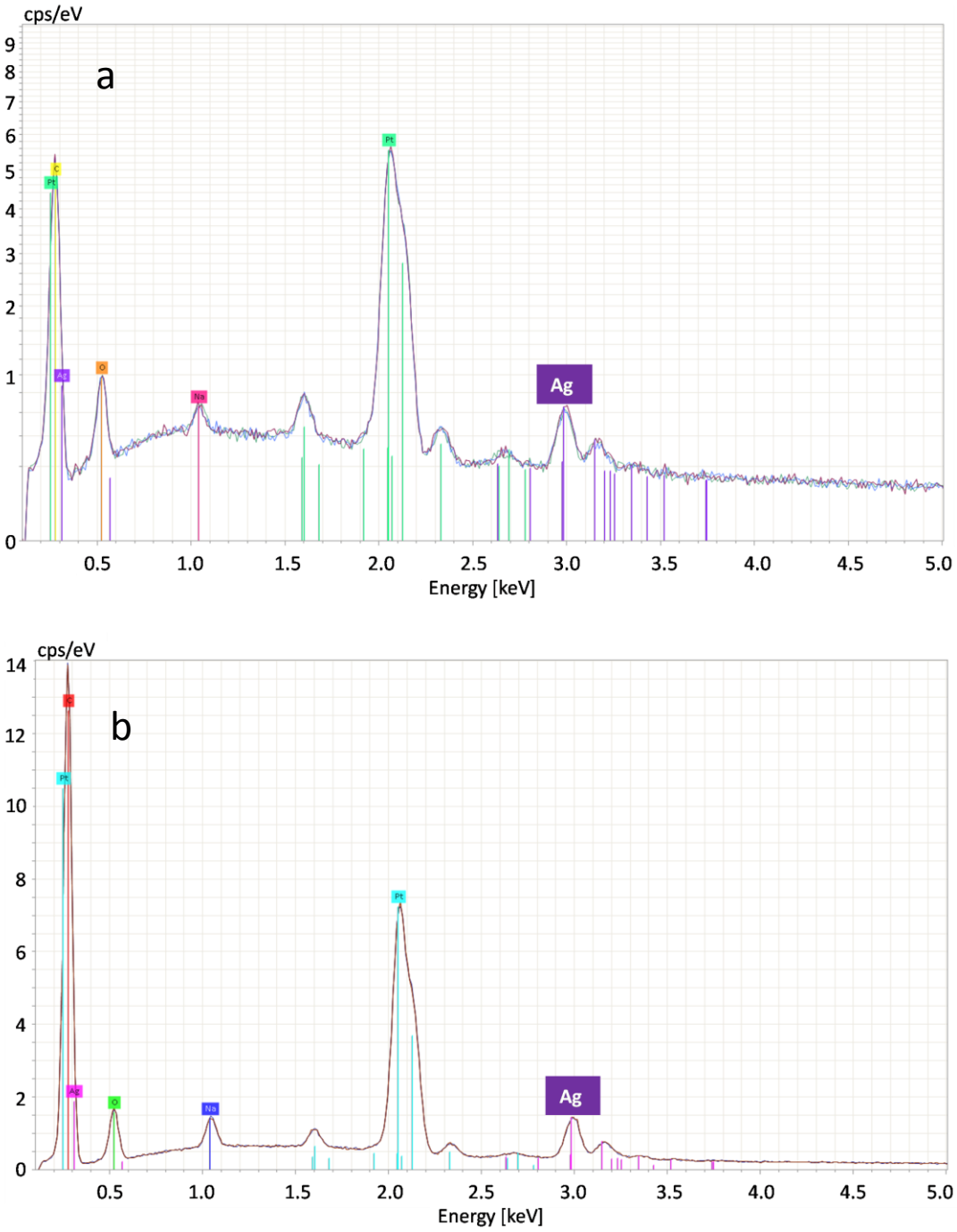

Figure 5 EDS analysis of (a) R film and (b) UV film.

4.6 Transmission electron microscopy (TEM) and cell membrane permeability test

Damages of bacteria treated with R and UV films are shown in Fig. 6. Compared to the normal cell morphology (control) in Fig.6a, the treated cells demonstrated cell leakage (Fig 6b,c). Tiny black dots shown in leakage cells are the AgNPs.

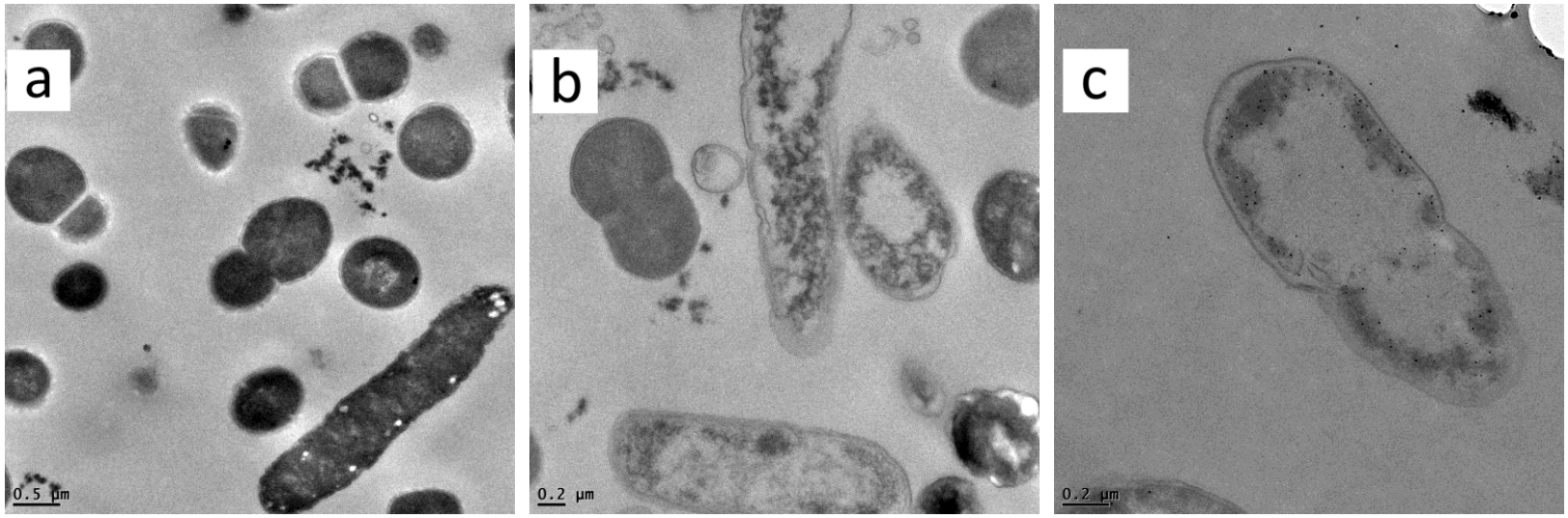

Figure 6 TEM images of *E. coli* (a) and *E. coli* treated with R (b) and UV film (c).

The result of the cell membrane permeability test is shown in Fig. 7. Significantly ($P \leq 0.05$) higher absorbance of DNA and protein were detected in the R and UV AgNP/BNC slurry treated samples. This indicated that the bacteria treated with the R and UV slurry underwent serious damage which resulted in a large amount of DNA and protein release. The results between the R and UV slurry treatments were not significantly different ($P > 0.05$).

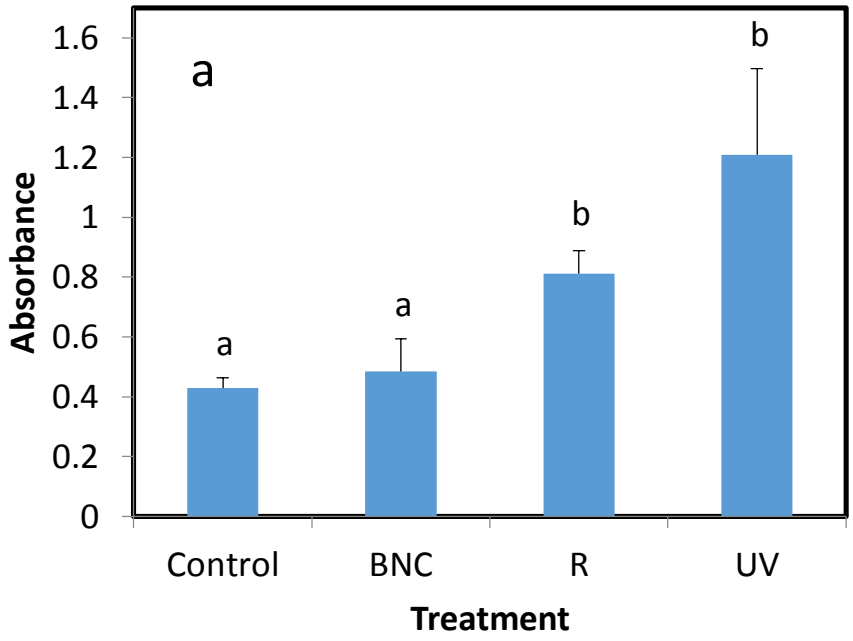

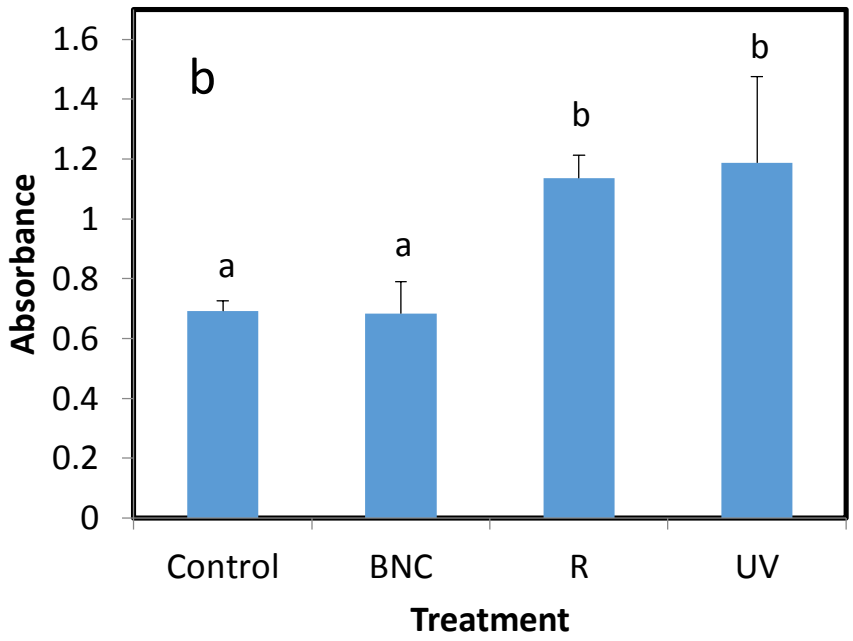

Figure 7 DNA (a) and protein (b) release of *E. coli* and *E. coli* treated with pure BNC and AgNP/BNC slurry made from R and UV method.

4.7 Water vapor transmission rate (WVTR)

The quantity of water vapor transmitted through a unit film during a definite time can be expressed by water vapor transmission rate (WVTR). A lower WVTR corresponds to a lower moisture transmission through the film and indicates a stronger water vapor holding ability. Fig. 8 shows the WVTR values of the PVA, PVA/BNC and AgNP/PVA/BNC films. Compared to the control group (4452.2 g/m^{2}day), the lowest WVTR (3444.7 g/m^{2}day) appeared in PVA/BNC film. A decreasing trend was observed when BNC appeared in the films, but differences between each sample were not significant ($P > 0.05$). No obvious difference was observed between the PVA/BNC film and AgNP/PVA/BNC film, and R and UV film.

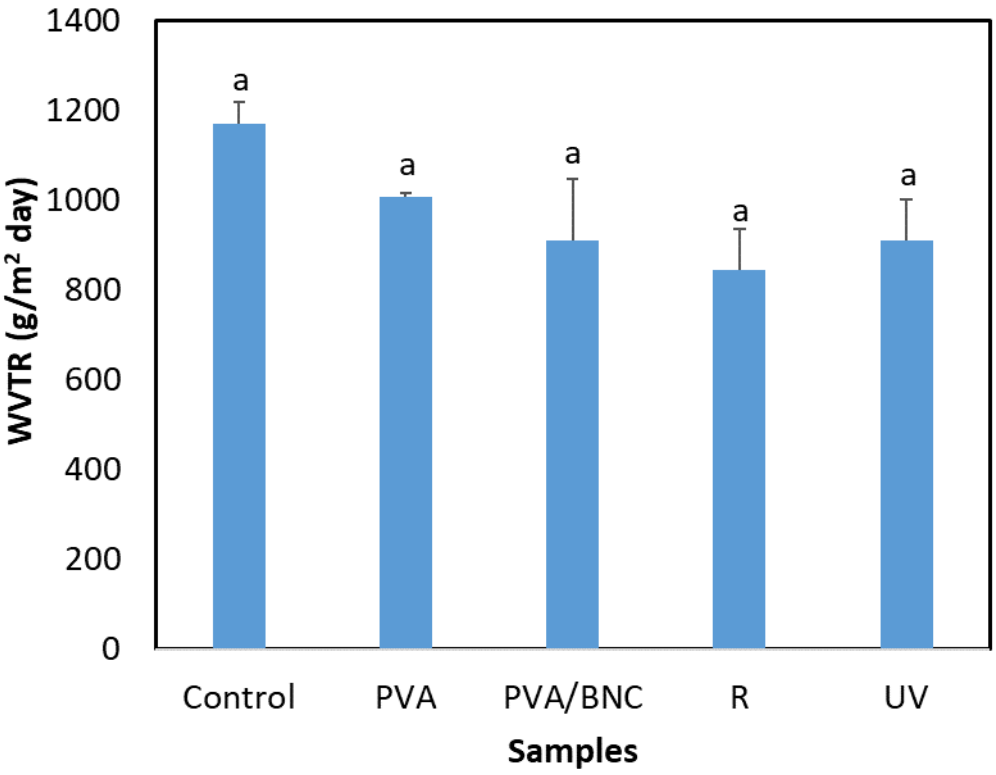

Figure 8 Water vapor transmission rate of AgNP/PVA/BNC films.

4.8 Oxygen barrier

A higher POV indicates a higher degree of oxidation, which relates to a lower oxygen barrier capacity. As shown in Fig. 9, the POV of corn oil covered by the films was significantly ($P \leq 0.05$) lower than that of the open jar group. In the film-covered groups, the BNC-based groups had significantly ($P \leq 0.05$) lower POV than the PVA group. The lowest POV appeared in the jar covered with the R film, but the difference between R and UV films is not obvious.

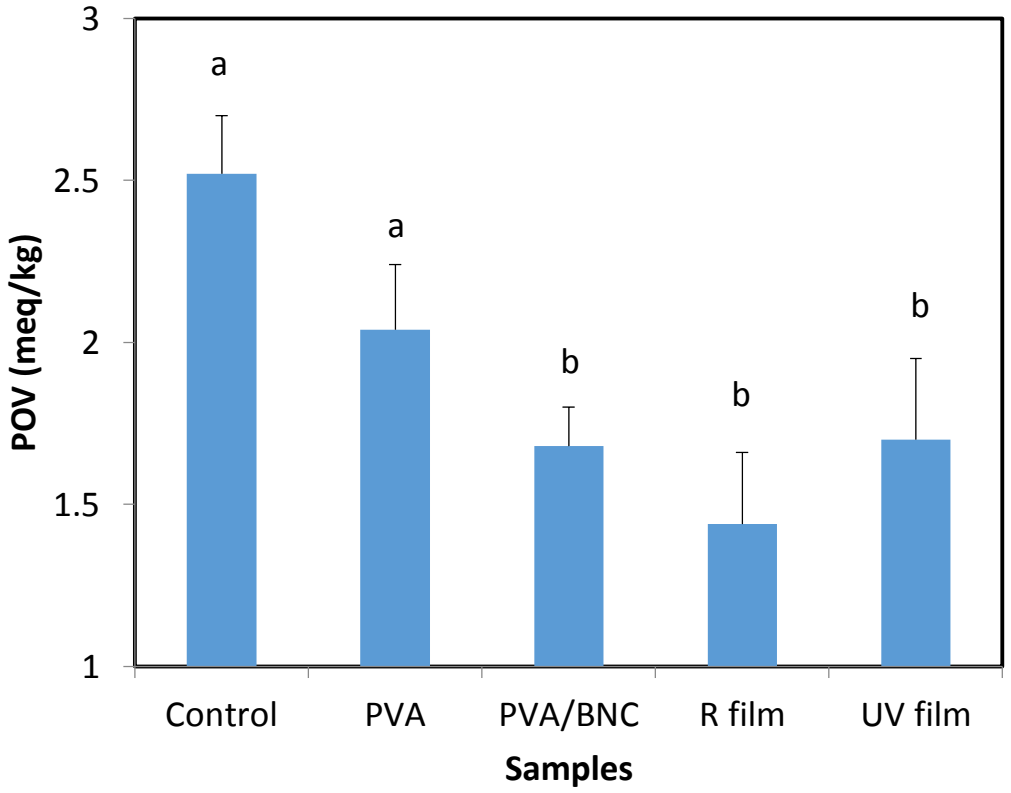

Figure 9 Oxygen barrier capacity of AgNP/PVA/BNC films.

4.9 Release test

The amount of silver released to physiological saline solution is shown in Fig. 10. At 0 h, almost no silver release was observed in R film while a 2.844 mg/m^2 silver release was detected in UV film. The longer the film soaked in solution, the greater the amount of silver released from the film. The silver release amount of the UV film is significantly higher than that of the R film at 3 and 24 h. The gap of silver release between the R and UV films narrowed as time increased.

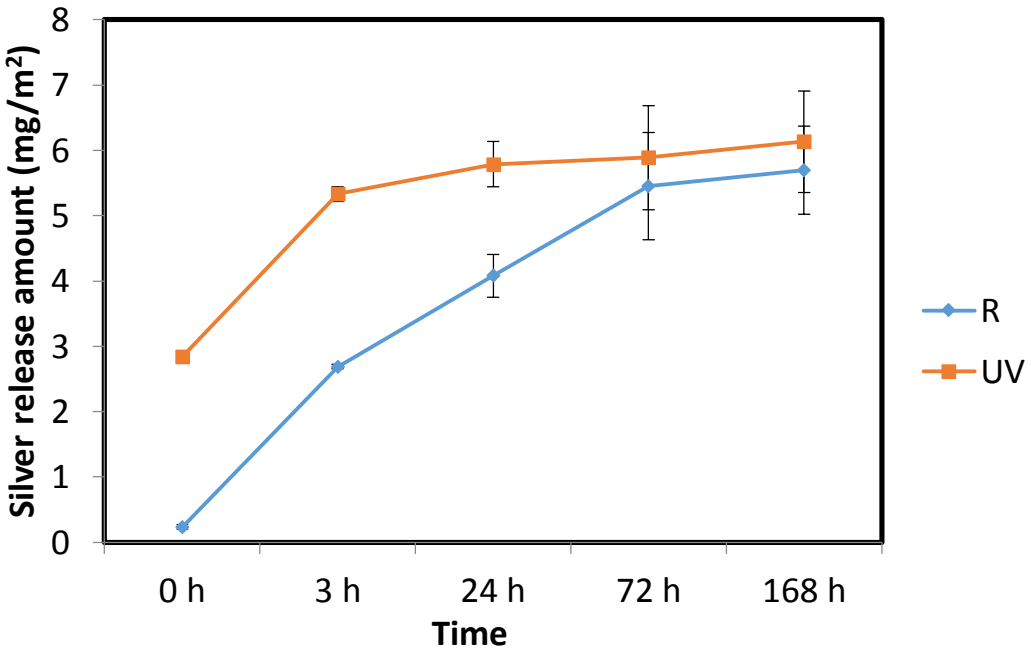

Figure 10 Silver release of AgNP/PVA/BNC films.

4.10 Bacterial inhibition test

The effect of the incorporation of AgNPs into the PVA/BNC film on *E. coli* O157:H7 growth is shown in Fig. 11. The bacteria in the control group increased by almost 6 log CFU/mL in 24 h. The growth pattern of the PVA/BNC group overlapped that of the control group, indicating that no bacterial reduction occurred. The R and UV films as treatment groups showed significant reductions ($P \leq 0.05$) during the 24-h incubation period. The UV film showed significantly ($P \leq 0.05$) greater antimicrobial activity than the R film from 3 to 24 h. Compared with the control group, 4.8 and 7.3 log CFU/mL reductions were observed in the R film and UV film, respectively.

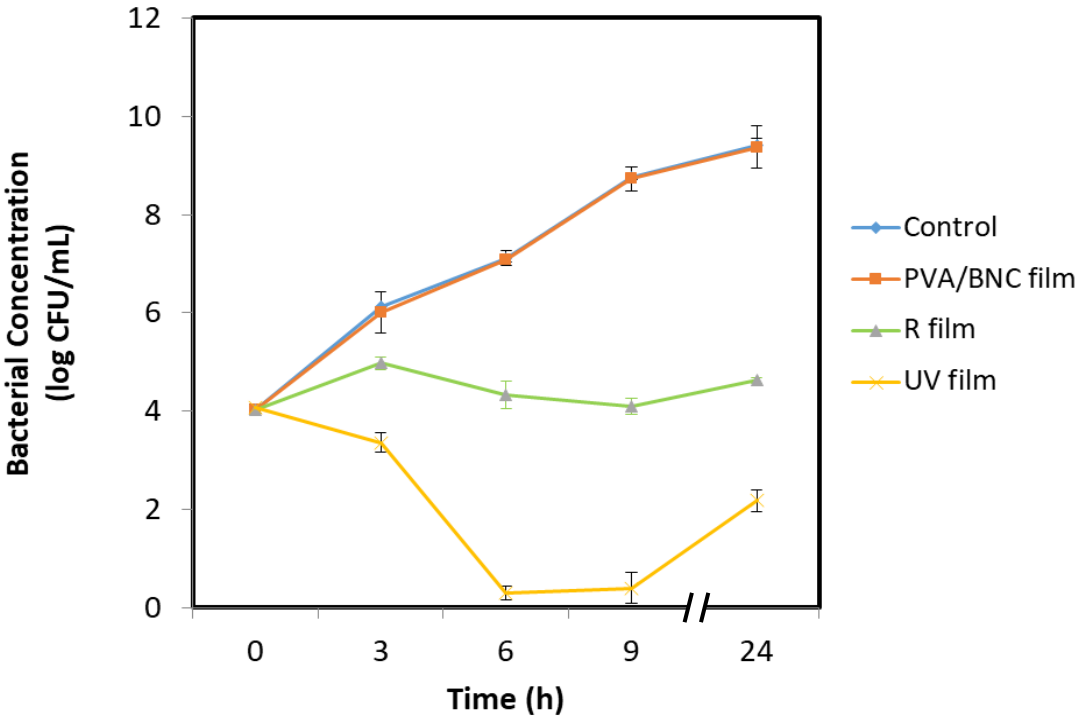

Figure 11 Inhibition of E. coli O157:H7 cocktail by BNC, R and UV films.

4.11 Beef shelf-life study

Fresh beef wrapped with the treatment films were stored at 4 ^{o}C to examine the change in total bacterial counts during refrigerated storage. The influence of AgNP/BNC/PVA film on the growth of bacteria on beef is presented in Fig. 12. Comparing to the control groups, both R film and UV film were capable of inhibiting bacterial growth from the beginning. Significant reductions were achieved from day 4 to day 10. After 10 days, the total bacterial count increased in both treatment and control groups, and the differences between each group were no longer significant ($P \leq 0.05$). The highest reduction appeared at day 7 where 3 log CFU/cm^2 of reduction was observed in beef wrapped with the UV film.

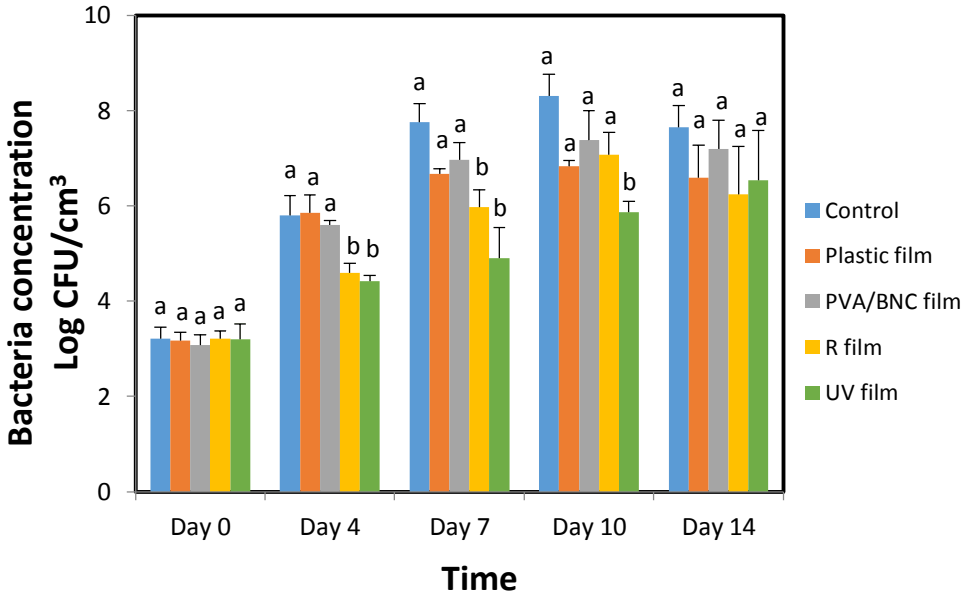

Figure 12 Inhibition of natural microorganisms on raw beef by plastic package, BNC, R and UV films.

4.12 Beef inoculation test

Beef inoculated with a five-strain *E. coli* O157:H7 cocktail was used to investigate the antimicrobial effect of AgNP/PVA/BNC films against this pathogen. As shown in Fig. 13, unlike the beef shelf-life test in which the bacteria were inhibited from the beginning, a significant ($P \leq 0.05$) decrease of bacterial concentration was only observed at day 7 since 8 logs CFU/cm^2 of bacteria were initially inoculated on the beef. This indicates that it takes more time for the AgNPs to inhibit the growth of *E. coli* O157:H7. A decreasing tendency appeared at day 4, and the biggest decrease (3 log) appeared at day 10. The plastic film and PVA/BNC film as controls failed to inhibit the growth of bacteria.

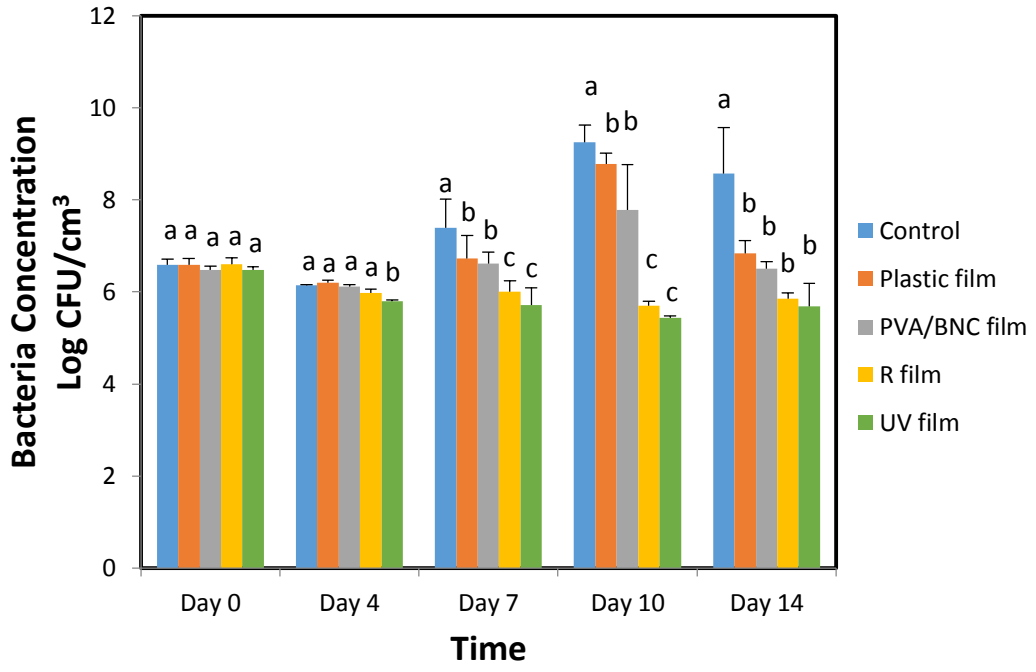

Figure 13 Inhibition of E. coli O157:H7 on raw beef by plastic package, BNC, R and UV films.

4.13 Toxicity against intestinal bacteria

The antimicrobial activity of AgNPs/BNC slurry against 5 intestinal bacteria was shown in Fig. 14. A six-log decline of *E. coli* concentration was observed, suggesting a high antimicrobial effect on normal Gram-negative bacteria. However, the inhibition of other strains was not significant. Under both aerobic and anaerobic conditions, the AgNPs/BNC slurry failed to inhibit the growth of *Lactobacillus* and *Bifidobacterium*.

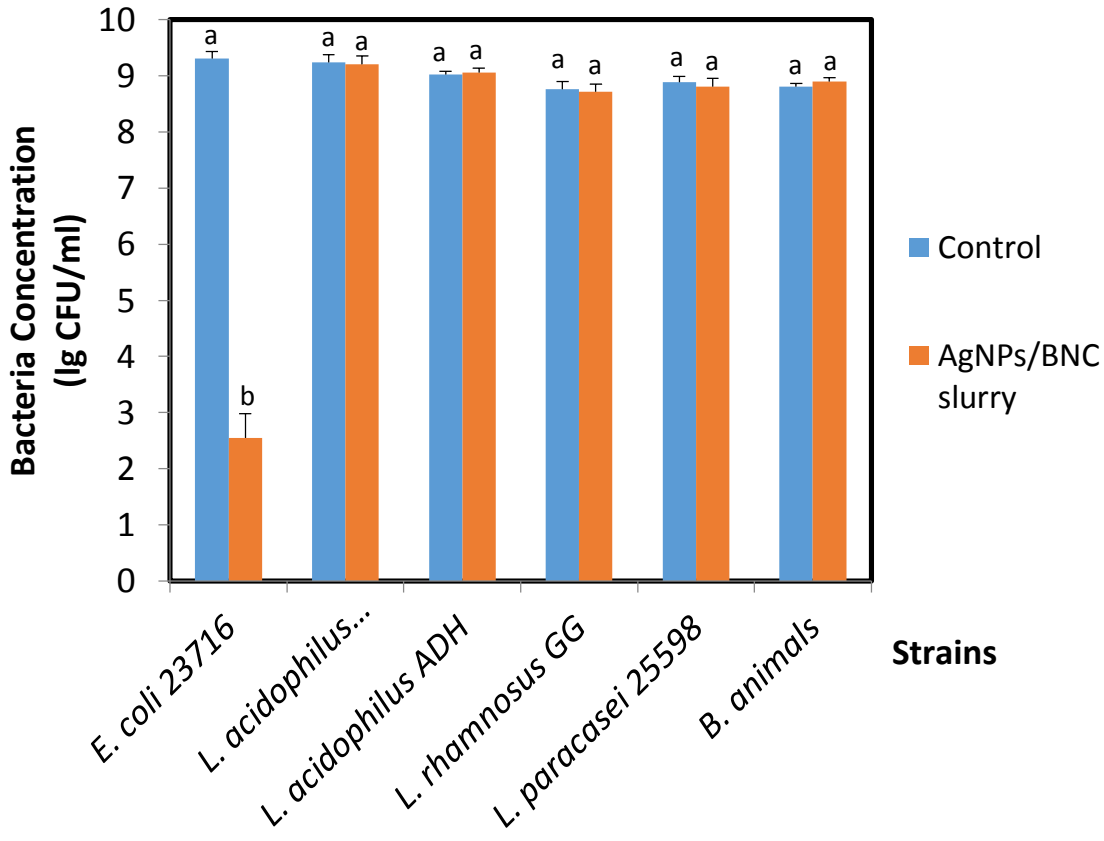

Figure 14 Toxicity against intestinal bacteria

4.14 Toxicity against Caco-2 cells

Caco-2 cells were exposed to UV and reduction generated AgNPs of different concentration. The cytotoxicities of AgNPs were evaluated by MTT assay and confirmed by WST assay. According to Figure 15, after 24 h exposure, the cell viability of Caco-2 cells treated with R AgNP/BNC slurry was 40% at 2000 μg/mL and 70-80 % at other concentrations. However, Caco-2 cells treated with UV AgNP/BNC slurry exhibited significantly ($P \leq 0.05$) lower cell viability at the concentration of 100 μg/mL and above. 70-80% cell viabilities only exhibited when the slurry concentration was lower than 50 μg/mL.

The same result was shown in the WST assay. Significant ($P \leq 0.05$) decreases of cell viability can be observed at 2000 μg/mL for R AgNP/BNC slurry and 100 μg/mL for UV AgNP/BNC slurry.

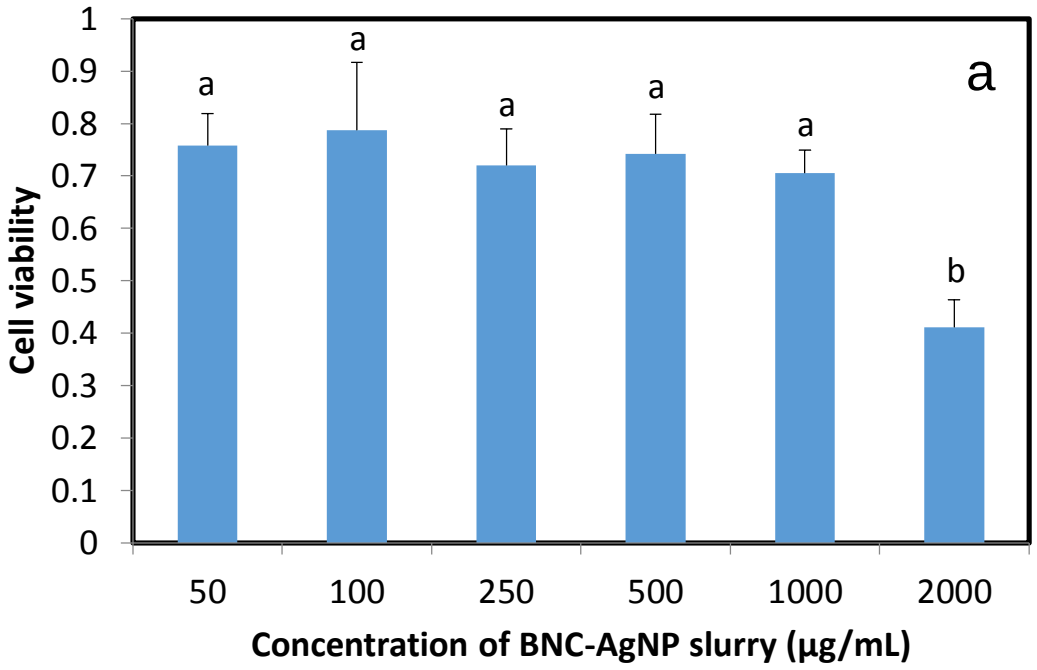

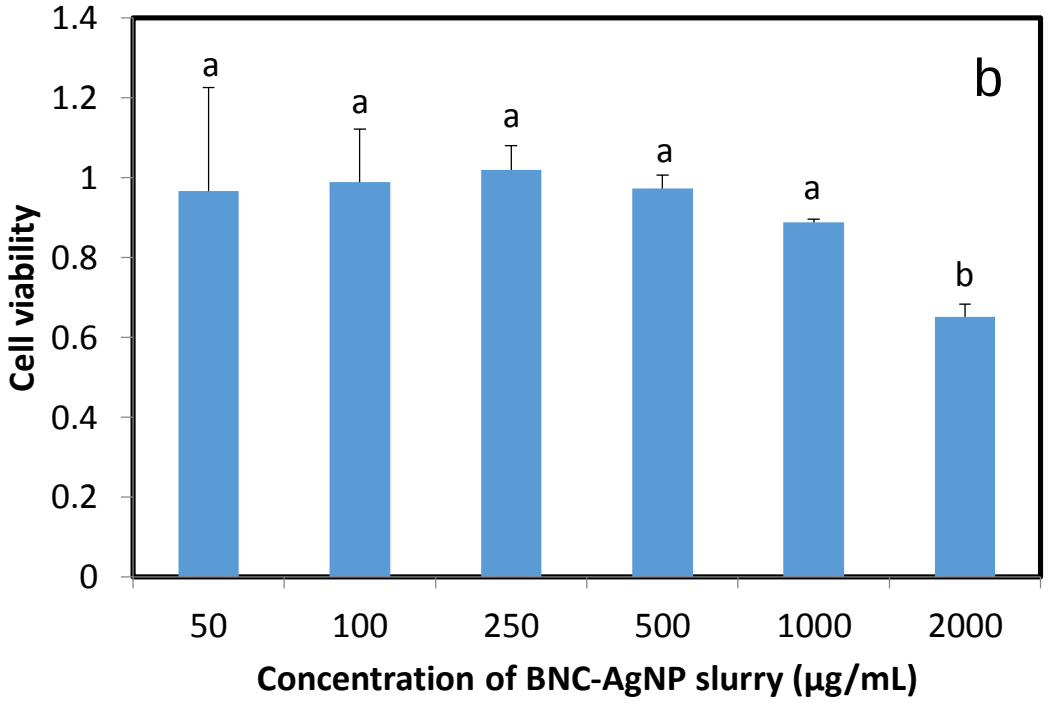

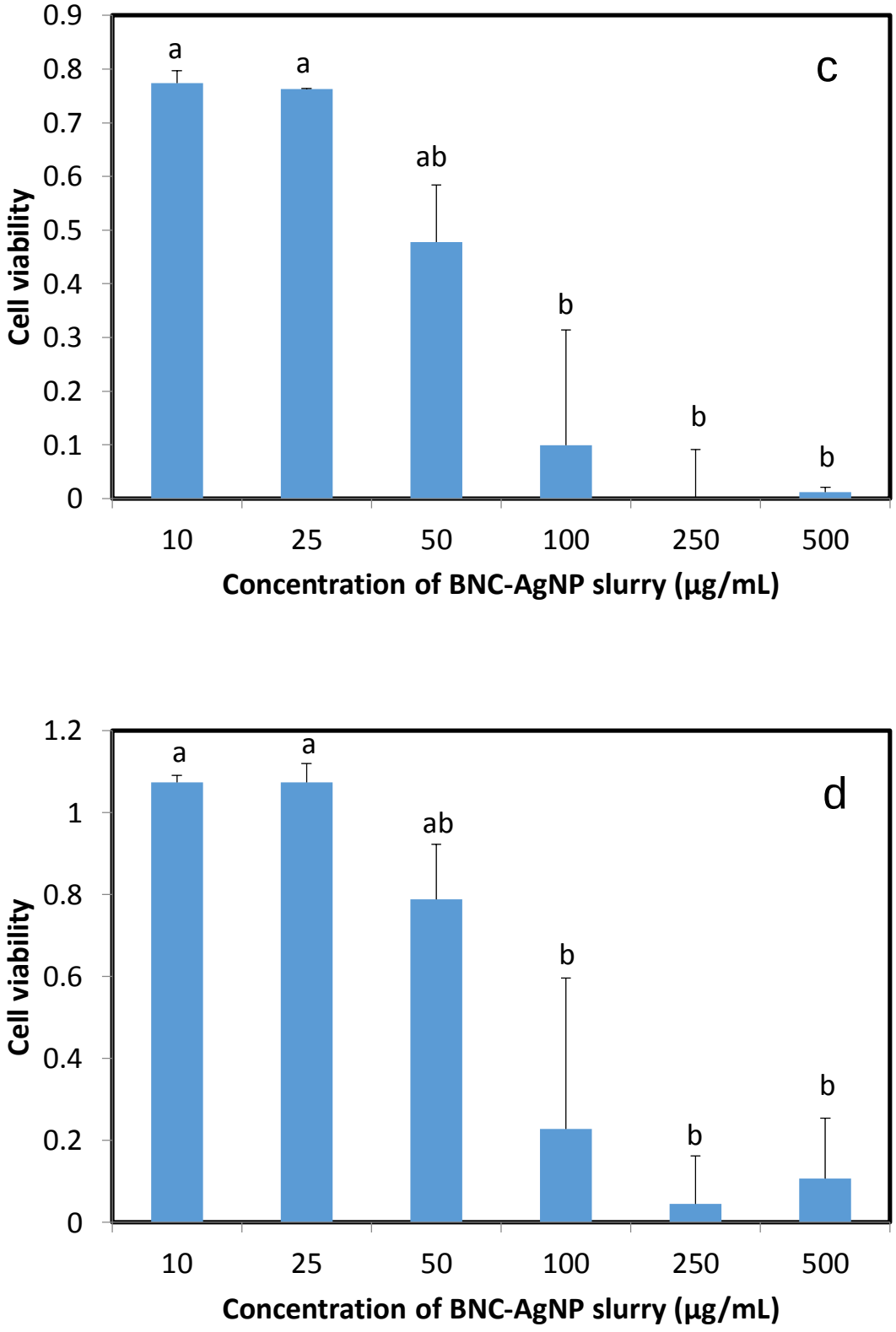

Figure 15 Toxicity of R film against Caco-2 cells tested by MTT (a) and WST assay (b) and UV film against Caco-2 cells tested by MTT (c) and WST assay (d).

4.15 Toxicity against FHC cells

As shown in Fig. 16, in the MTT assay, the FHC cells exhibited significant ($P \leq 0.05$) cell death when treated with 1000 μg/mL or higher concentration of R AgNP/BNC slurry, and almost no cell viability when treated with 100 μg/mL or higher concentration of UV AgNP/BNC slurry. Mild but not significant cell viability reduction was observed at the slurry concentration between 10 and 50 μg/mL.

The WST assay showed similar result (Fig 16b & d). FHC cells were inhibited by R AgNP/BNC slurry at 2000 μg/mL but only 50 μg/mL by UV AgNP/BNC slurry.

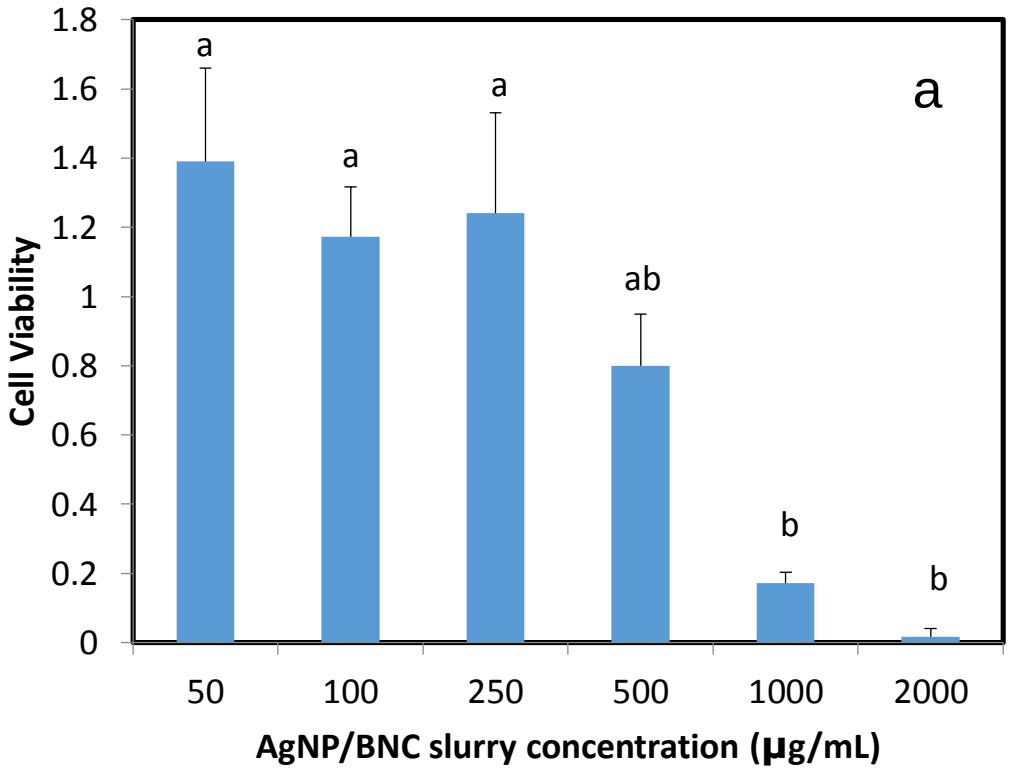

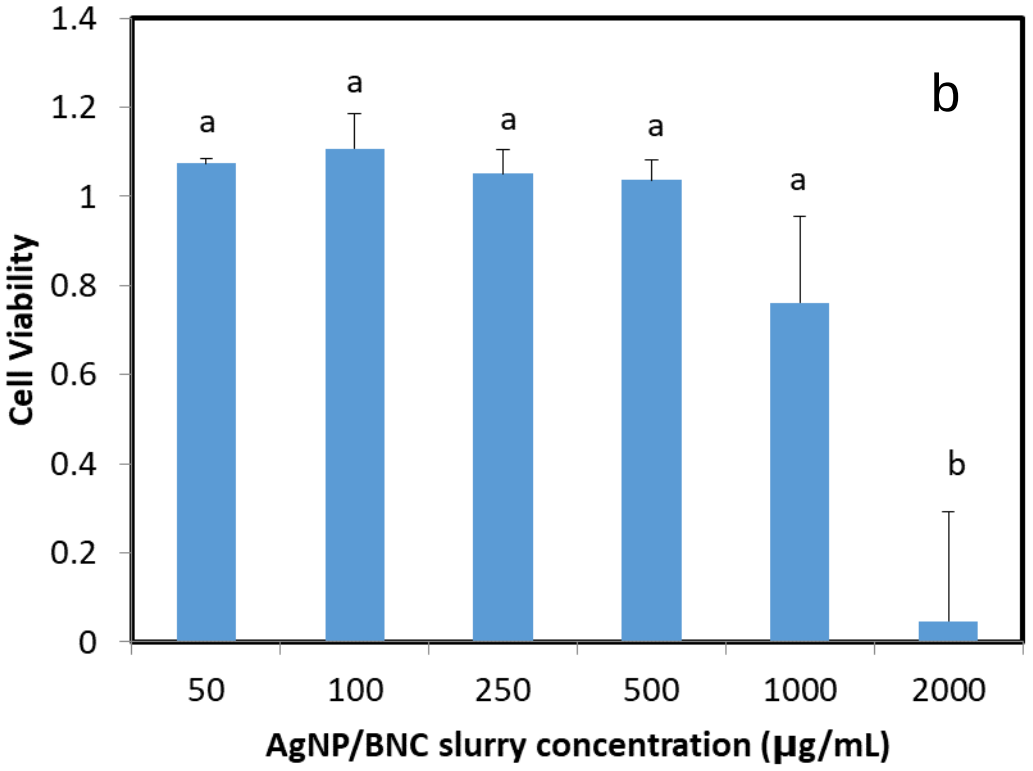
b
Cell Viability
1.4
1.2
1
0.8
0.6
0.4
0.2
0
a
a
a
a
a
b
50
100
250
500
1000
2000
AgNP/BNC slurry concentration (µg/mL)

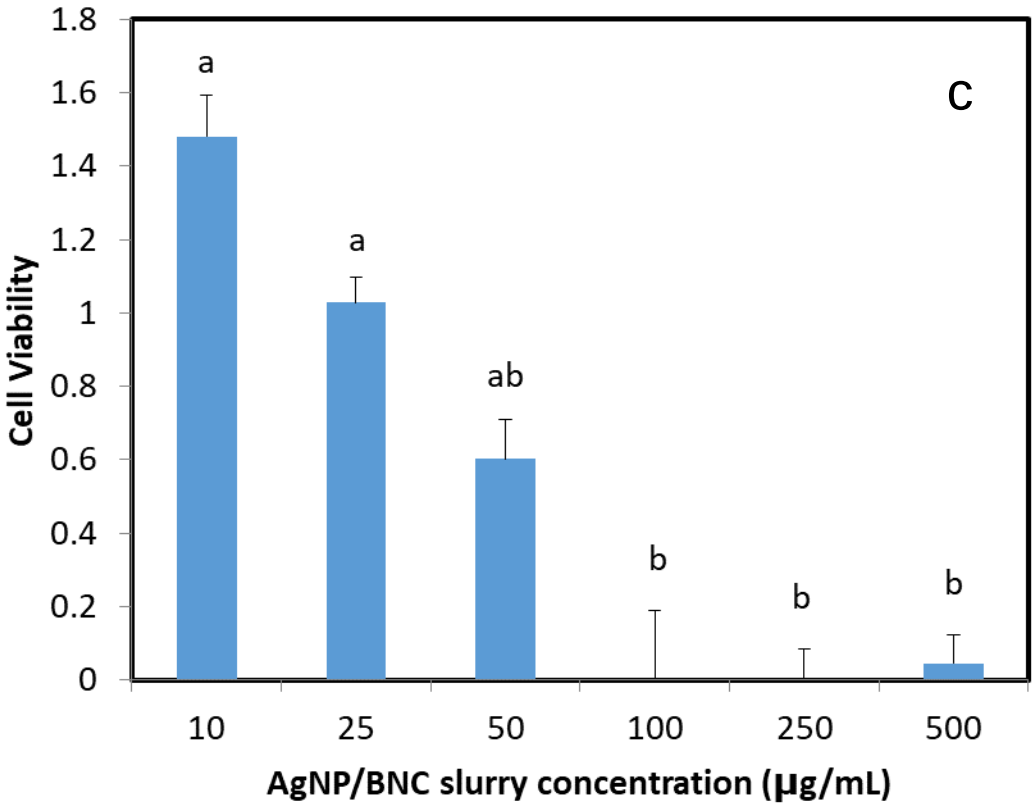
c
Cell Viability
1.8
1.6
1.4
1.2
1
0.8
0.6
0.4
0.2
0
a
a
ab
b
b
b
10
25
50
100
250
500
AgNP/BNC slurry concentration (µg/mL)

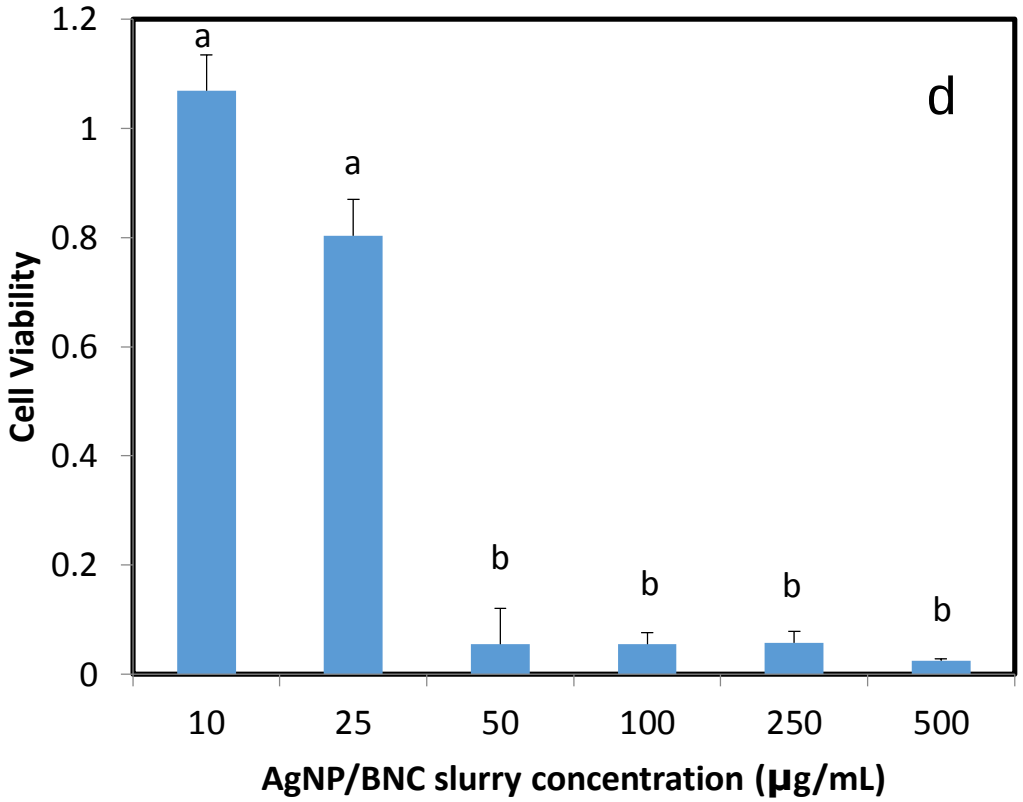

Figure 16 Toxicity of R film against FHC cells tested by MTT (a) and WST assay (b) and UV film against FHC cells tested by MTT (c) and WST assay (d).

CHAPTER 5 DISCUSSION

5.1 AgNPs synthesis

In the reduction method, an excess of $NaBH_4$ was needed to reduce the Ag^+ ions. $NaBH_4$, as a strong reducing agent, reduced $AgNO_3$ through the chemical reaction (Mulfinger and others 2007):

$$AgNO_3 + NaBH_4 \rightarrow Ag + 1/2H_2 + 1/2B_2H_6 + NaNO_3$$

BNC as stabilizer promoted the formation of AgNPs.

The UV method is considered as a green method for synthesizing AgNPs. In this method, the BNC acted as a particle stabilizer and the inter- and intra- hydroxyl groups in the glucose unit of BNC played the role of reducing agent. When BNC was immersed in silver nitrate solution, the Ag^+ ions adsorbed and diffused into the cellulose fibers due to a strong electrostatic force between Ag^+ ions and the hydroxyl groups of BNC molecule (He and others 2003). After being exposed to UV light, the $–CH_2(OH)$ groups in the BNC structure were converted to aldehyde groups (–CHO) which directly reduced Ag^+ into Ag^o and were, in turn, oxidized into carboxyl groups (–COO-). The amorphous Ag^o clustered on BNC fibers surface and crystallized to form spherical AgNPs. The synthesized AgNPs were finally stabilized by the stearic effect of the fiber chains (Li and others 2015; Emam and others 2014; Rehan and others 2017).

5.2 Color

PVA is a nontoxic biodegradable polymer that exhibits excellent chemical resistance, water absorption, gas barrier and film-forming properties (Thong and others 2016; DeMerlis and Schoneker 2003). The PVA/BNC film became translucent because of the dilution of BNC slurry by the colorless PVA solution. The brown color of the AgNP/PVA/BNC film is caused by AgNPs which is yellowish-brown due to the surface plasmon resonance (SPR) (Liz-Marzán 2004). AgNPs dispersed into the film and greatly affected the color of the film. The same effect was found by Rhim and others (2013).

5.3 Mechanical properties

The improvement of mechanical properties in the AgNP/PVA/BNC film can be explained by the addition of PVA. Good physical properties and antimicrobial activity have been observed in AgNP-modified PVA film (He and others 2017). When BNC was modified by PVA, the closely-linked glucose polymers of BNC were broken by physical force and reconnected by the PVA solution. Once the solution solidified, the flexibility of PVA would apply to the PVA/BNC film. AgNPs as metallic nanoparticles did not affect the mechanical properties of the film.

5.4 Fourier transform infrared (FTIR) spectra

In the FTIR spectra, the addition of PVA smoothed the peak at 3300 cm^{-1} and split the peak at 2900 cm^{-1}. This is probably due to the O–H stretch of the

intermolecular and intramolecular hydrogen bonds in PVA which broadens the band (González-Guisasola and Ribes-Greus 2018). Moreover, the spectral pattern of BNC is retained in the spectra of PVA/BNC and AgNP/PVA/BNC film, which suggested that AgNPs were not chemically connected to the PVA/BNC matrix. The addition of AgNPs did not show any effect on BNC absorption.

5.5 UV-vis spectra

The formation of AgNPs was confirmed by the absorption band at 410 nm in the UV-vis absorption spectra of AgNP/BNC slurry made by the reduction method. However, no absorption band was obtained in the AgNP/BNC slurry made by the UV method, probably due to the fact that the AgNPs tightly bound with the BNC fibers and the released AgNPs were not concentrated enough to be detected. A higher amount of AgNPs is required to be detected by UV-vis spectra (Kanmani and Rhim 2014).

5.6 Scanning electron microscopy (SEM) and energy dispersive X-ray spectroscopy (EDS)

The surface structure of films was observed through SEM. The fiber network of BNC slurry is looser than the original BNC since it had been blended and part of the links were damaged. AgNPs synthesized in the reduction and UV methods are similar in shape and size, but a higher concentration of AgNPs was obtained in the UV method due to a higher concentration of $AgNO_3$ solution used in the film-making

step.

5.7 Water vapor transmission rate (WVTR)

Low WVTR is expected in the food packaging film to reduce the moisture transmission between food and environment. The lower WVTR observed in BNC based films indicated that the addition of BNC has a potential ability to improve the water vapor barrier capability of the PVA films. This can be confirmed by previous studies that the WVTR of PVA and other plastic packaging decreased with the increase in BNC addition (Spence and others 2011; Chiulan and others 2018). The decrease of WVTR is probably due to a good PVA/BNC interface which reduces the chain mobility (Chiulan and others 2018) and the highly absorbent microstructure of BNC.

AgNPs did not show any effect on WVTR. A similar result was reported by Kanmani and Rhim (2014). However, Rhim and others (2013) reported that WVTR decreases with the incorporation of AgNPs, which might be related with the increased tortuous pathway caused by the AgNPs incorporated in the film. The concentration of AgNPs in this study is not high enough to significantly affect the WVTR.

5.8 Oxygen barrier

POV is much lower in the film-covered groups since oxygen was blocked by the films to a certain degree. A lower POV was detected in groups of BNC-based films, leading to the conclusion that the BNC acted as an effective oxygen barrier. The

positive effect of BNC on oxygen barrier ability can be explained by its dense network structure. The inherent flexibility of BNC could reduce the spaces between the fibrils and narrow the path of oxygen (Ferrer and others 2017).

5.9 Release test

A large amount of silver was released from both R and UV films in the first three hours. This could be a surface release, in which the superficial AgNPs are easy to escape from the film surface since the blocking effect is weak. To the contrary, after 3 h, when release happened within the film, silver was released much slower because of the interactions between AgNPs and the PVA/BNC mixture, and the blocking effect of BNC networks (Yang and others 2012a). A difference of silver release rate between the R and UV films was observed. The silver release from the UV film is higher than the R film at all times because a higher concentration of $AgNO_3$ was used in the film-making step. As shown in Fig. 10, the AgNP/PVA/BNC film continued releasing silver for up to 7 days and probably beyond. This helped to maintain an antibacterial activity for a long term, which promoted its application as an antimicrobial food packaging.

5.10 Bacterial inhibition test

The reduction of bacterial numbers in treatment groups confirmed the antimicrobial activity of AgNPs. The AgNPs released from the films killed the bacteria by either breaking the cell walls using electrostatic attraction between the

positively charged nanoparticles and negatively charged bacterial cells (Hamouda and Baker 2000), or destroying the DNA and protein function of bacteria cells (Feng and others 2000). This can be confirmed by the result of nucleic acid release test and TEM images. A bigger reduction was observed in the UV film group. This can be explained by a higher AgNPs release rate which was confirmed by the ICP results (Fig. 10). Moreover, the growth curve of R and UV groups rose at the end of the 24 h (Fig. 11). This indicated that AgNPs only inhibited the growth of the bacteria, instead of killing the bacteria.

5.11 Beef shelf-life

In the beef shelf-life experiment, resident bacteria were inhibited until day 10, suggesting that the presence of AgNPs effectively inhibited the growth of bacteria on raw beef for at least 10 days at 4 ^{o}C. At day 4 and 7, the total bacterial count in the UV film group was significantly lower than that in the R film group, indicating a higher antimicrobial ability of the UV film. Similarly, AgNP-modified films were also reported to prolong the shelf-life of sausages (Marchiore and others 2017) and fresh-cut carrots (Costa and others 2012).

Furthermore, the bacterial inhibition process on raw beef is slower than that in the pure culture, mainly because of two reasons. Firstly, the inhibition only took place on the beef surface which is in direct contact with the film, and secondly, the microflora on raw beef include populations of Gram-positive and Gram-negative bacteria which are much more complex than the pure culture of *E. coli* O157:H7 alone. In fact,

Gram-positive bacteria were reported show higher resistance to antibiotics than Gram-negative bacteria due to their cell wall structure (Pelgrift and Friedman 2013).

5.12 Beef inoculation test

AgNPs showed a high antimicrobial ability against *E. coli* O157:H7 *in vitro*, which also appeared to apply to inoculated beef samples. According to the results, the AgNP/PVA/BNC film is able to keep the number of *E. coli* at 1 log lower than the original number for two weeks. The UV film group had a lower bacterial concentration than the R group at all time points, which indicated that the UV film has a relatively higher antimicrobial activity than the R film (Fig. 13). This result is consistent with those of the experiments conducted above.

Compared to the pure bacterial culture, the bacteria inoculated on raw beef were less sensitive to AgNPs. This is probably due to the complex food components that conferred a protective effect to the bacteria. Similar result was reported by Azlin-Hasim and others (2016) and Cruz-Romero and others (2013). As Azlin-Hasim reported, Ag^{+} would bind with the protein functional groups of the raw beef and weaken the antimicrobial activity of AgNPs.

5.13 Toxicity against intestinal bacteria

Compared to *E. coli* which showed high sensitivity to AgNPs, strains of *Lactobacillus* and *Bifidobacterium* were not affected by AgNPs. This can be explained by the difference between Gram-positive and Gram-negative bacteria.

Gram-positive bacteria have a thicker cell wall that contains a large amount of peptidoglycan (Muthuvel and others 2014) which impede the penetration of AgNPs. In contrast, *Lactobacillus bulgaricus* and *Lactobacillus casei* were reported to be more susceptible to AgNPs than *E. coli* (Tian and others 2018). They claimed that the acidic environment produced by *Lactobacillus* promoted AgNPs diffusion. However, behavior of each bacterium depended on their metabolic characteristics. Some *Lactobacillus* and *Bifidobacterium* as Gram-positive bacteria have stronger cell wall and are more resistant to silver ions. Previous studies also reported that AgNPs exhibited higher antimicrobial activity on Gram-negative bacteria than Gram-positive ones (Mandal and others 2016).

5.14 Toxicity against Caco-2 cells

In this study, the cytotoxicity of AgNPs prepared by R and UV methods were studied by MTT and WST assay. The viability of Caco-2 cells considerably decreased with increasing the concentration of AgNPs. Almost no cell survive when the AgNP concentration is higher than 100 μg/mL, but no significant cytotoxicity effect was observed at lower AgNP concentration, which indicated that the inhibitory concentration of UV synthesized AgNPs against Caco-2 cells is 100 μg/mL in 24 h. Similar result was reported on Human epithelial carcinoma cell line (HeLa) (Sukirtha and others 2012). However, the cells treated with reduction synthesized AgNPs was inhibited only when the AgNP concentration is higher than 2000 μg/mL. This is probably because of the higher concentration of $AgNO_3$ used in the preparation of UV

AgNP/BNC slurry, and a larger amount of AgNPs were synthesized. The toxicity of AgNPs can be explained by the production of reactive oxygen species (ROS) which plays important role in cell signaling and homeostasis (Devasagayam and others 2004). The increase of ROS will lead to significant damage to cell structures and further caused apoptosis and necrosis, forms of uncontrolled cell death for cancer cells (Hampton and Orrenius 1997). AgNPs are able to enter cells, locate in several cell organelles and promote the production of ROS, and thus have the potential application in cancer therapeutics (Chung and others 2016). Moreover, the AgNPs used in this study have a size around 30 nm. The toxicity of AgNPs is critically determined by the NPs size. As reported by Avalos, AgNPs with smaller size have higher toxicity than larger ones since they can more easily enter the cells and promote ROS generation (Avalos and others 2014). Other explanations of AgNPs toxicity include the physicochemical interactions between silver ions and intracellular protein of cells (Heydari and Rashidipour 2015) and the expression of syncytin-1 mRNA which can promote the fusion of malignant cells (Bjerregaard and others 2006).

5.15 Toxicity against FHC cells

Similar growth rate reductions were observed in FHC cells. The inhibitory concentration of AgNPs against Caco-2 cells is 50 μg/mL for UV synthesized AgNPs and 1000 μg/mL for reduction synthesized AgNPs. Compared with Caco-2 cells, FHC cells in this study seem to be more sensitive to AgNPs, leading to a speculation that normal cells have lower tolerance to AgNPs than cancer cells. However, a higher

toxicity of Pt/folate NPs was reported against breast cancer cells rather than normal cells (Mironava and others 2013), and a selective internalization of into cancer cells was reported which means cancer cells are more easily to be exposed to NPs (Lojk and others 2018). In this study, the experiments of AgNPs against cancer cells and normal cells were conducted separately and incomparable. Further studies are needed to understand the difference of AgNPs working mechanism between cancer and normal cells.

CHAPTER 6 CONCLUSIONS

In this study, PVA and AgNPs were incorporated in BNC to develop AgNP/PVA/BNC films through reduction and UV methods. AgNPs changed the color of film from white to brown while not chemically affecting the films' surface structure. The mechanical property of the film was enhanced due to the addition of PVA. The oxygen barrier capacity was improved because of the dense network structure of BNC. A tendency of decreasing WVTR was also observed but more studies are needed to confirm. The films were able to inhibit the growth of *E. coli* O157:H7 in broth and on raw beef, and effectively control the number of natural bacteria on raw beef, providing a potential method to prolong beef shelf-life. UV films exhibited stronger antimicrobial properties than R films in all antimicrobial experiments. Inaddition, the toxicity test indicated that the AgNPs were nontoxic to intestinal bacteria and showed toxicity to human cells only when the concentration is higher than 1000 μg/mL for reduction synthesized AgNPs and 50 μg/mL for UV synthesized AgNPs.

This research provided two methods of preparing AgNP/PVA/BNC films. In the reduction method, the size of AgNPs is greatly affected by the concentration of the two chemical reagents ($AgNO_3$ and $NaBH_4$). A low chemical concentration is required to form AgNPs with the desired size, thus, the reduction method is limited to low AgNP production. On the contrary, the formation of AgNPs in the UV method depends on UV irradiation, and a higher concentration of AgNPs can be obtained by increasing the concentration of $AgNO_3$. Therefore, 0.1 M of $AgNO_3$ was used in the

UV method while only 0.01 M $AgNO_3$ was used in the reduction method, and the UV film exhibited a higher antimicrobial ability than the R film. As antimicrobial packaging, UV film has advantages over R film. However, a higher toxicity of UV film was also observed in human cells. The choice of film will be decided in different situations.

Altogether, the AgNP/PVA/BNC films are much more flexible than the pure BNC film. The great mechanical property makes it suitable to be used as packaging films in daily life. The materials of this film are biodegradable and will help to reduce environmental pollutions. Their excellent antimicrobial ability showed great potential in the application of food packaging.

REFERENCES

Abou-Yousef H, Saber E, Abdel-Aziz MS, Kamel S. 2018. Efficient alternative of antimicrobial nanocomposites based on cellulose acetate/Cu-NPs. Soft Materials:1-10.

Ahmad A, Mukherjee P, Senapati S, Mandal D, Khan MI, Kumar R, Sastry M. 2003. Extracellular biosynthesis of silver nanoparticles using the fungus *Fusarium oxysporum*. Colloids and Surfaces B: Biointerfaces 28(4):313-8.

Alila S, Ferraria AM, do Rego AMB, Boufi S. 2009. Controlled surface modification of cellulose fibers by amino derivatives using N, N′-carbonyldiimidazole as activator. Carbohydrate Polymers 77(3):553-62.

An D-S, Kim Y-M, Lee S-B, Paik H-D, Lee D-S. 2000. Antimicrobial low density polyethylene film coated with bacteriocins in binder medium. Food Science and Biotechnology 9(1):14-20.

ANSAY SE, Darling KA, Kaspar CW. 1999. Survival of *Escherichia coli* O157: H7 in ground-beef patties during storage at 2,− 2, 15 and then− 2 C, and− 20 C. Journal of Food Protection 62(11):1243-7.

Appendini P, Hotchkiss JH. 2002. Review of antimicrobial food packaging. Innovative Food Science & Emerging Technologies 3(2):113-26.

Ashjaran A, Yazdanshenas ME, Rashidi A, Khajavi R, Rezaee A. 2013. Overview of bio nanofabric from bacterial cellulose. Journal of the Textile Institute 104(2):121-31.

Austin LA, Kang B, Yen C-W, El-Sayed MA. 2011. Nuclear targeted silver nanospheres perturb the cancer cell cycle differently than those of nanogold. Bioconjugate Chemistry 22(11):2324-31.

Avalos A, Haza AI, Mateo D, Morales P. 2014. Cytotoxicity and ROS production of manufactured silver nanoparticles of different sizes in hepatoma and leukemia cells. Journal of Applied Toxicology 34(4):413-23.

Awwad AM, Salem NM, Abdeen AO. 2012. Biosynthesis of silver nanoparticles using Olea europaea leaves extract and its antibacterial activity. Nanoscience and Nanotechnology 2(6):164-70.

Azlin-Hasim S, Cruz-Romero MC, Morris MA, Padmanabhan SC, Cummins E, Kerry JP. 2016. The potential application of antimicrobial silver polyvinyl chloride nanocomposite films to extend the shelf-life of chicken breast fillets. Food and Bioprocess Technology 9(10):1661-73.

Bae S, Sugano Y, Shoda M. 2004. Improvement of bacterial cellulose production by addition of agar in a jar fermentor. Journal of Bioscience and Bioengineering 97(1):33-8.

Baek Y-W, An Y-J. 2011. Microbial toxicity of metal oxide nanoparticles (CuO, NiO, ZnO, and Sb2O3) to *Escherichia coli*, *Bacillus subtilis*, and *Streptococcus aureus*. Science of the Total Environment 409(8):1603-8.

Barlow C, Morgan D. 2013. Polymer film packaging for food: An environmental

assessment. Resources, Conservation and Recycling 78:74-80.
Basuny M, Ali IO, El-Gawad AA, Bakr MF, Salama TM. 2015. A fast green synthesis of Ag nanoparticles in carboxymethyl cellulose (CMC) through UV irradiation technique for antibacterial applications. Journal of Sol-Gel Science and Technology 75(3):530-40.
Berndt S, Wesarg F, Wiegand C, Kralisch D, Müller FA. 2013. Antimicrobial porous hybrids consisting of bacterial nanocellulose and silver nanoparticles. Cellulose 20(2):771-83.
Bjerregaard B, Holck S, Christensen IJ, Larsson L-I. 2006. Syncytin is involved in breast cancer-endothelial cell fusions. Cellular and Molecular Life Sciences CMLS 63(16):1906-11.
Blaker JJ, Lee K-Y, Li X, Menner A, Bismarck A. 2009. Renewable nanocomposite polymer foams synthesized from Pickering emulsion templates. Green Chemistry 11(9):1321-6.
Bohlmann GM. 2005. General characteristics, processability, industrial applications and market evolution of biodegradable polymers. Handbook of Biodegradable Polymers, Rapra Technology Ltd, Shawbury, UK:183-212.
Brayner R, Ferrari-Iliou R, Brivois N, Djediat S, Benedetti MF, Fiévet F. 2006. Toxicological impact studies based on Escherichia coli bacteria in ultrafine ZnO nanoparticles colloidal medium. Nano Letters 6(4):866-70.
Brown AJ. 1886. XLIII.—On an acetic ferment which forms cellulose. Journal of the Chemical Society, Transactions 49:432-9.
Cao H, Liu X, Meng F, Chu PK. 2011. Biological actions of silver nanoparticles embedded in titanium controlled by micro-galvanic effects. Biomaterials 32(3):693-705.
Cascone M, Maltinti S, Barbani N, Laus M. 1999. Effect of chitosan and dextran on the properties of poly (vinyl alcohol) hydrogels. Journal of Materials Science: Materials in Medicine 10(7):431-5.
Chawla PR, Bajaj IB, Survase SA, Singhal RS. 2009. Microbial cellulose: fermentative production and applications. Food Technology & Biotechnology 47(2).
Chen C-H, Chen S-H, Shalumon K, Chen J-P. 2015. Dual functional core–sheath electrospun hyaluronic acid/polycaprolactone nanofibrous membranes embedded with silver nanoparticles for prevention of peritendinous adhesion. Acta Biomaterialia 26:225-35.
Chen Y-H, Yeh C-S. 2002. Laser ablation method: use of surfactants to form the dispersed Ag nanoparticles. Colloids and Surfaces A: Physicochemical and Engineering Aspects 197(1-3):133-9.
Chiulan I, Frone AN, Panaitescu DM, Nicolae CA, Trusca R. 2018. Surface properties, thermal, and mechanical characteristics of poly (vinyl alcohol)–starch‐bacterial cellulose composite films. Journal of Applied Polymer Science 135(6).
Chung I-M, Park I, Seung-Hyun K, Thiruvengadam M, Rajakumar G. 2016. Plant-mediated synthesis of silver nanoparticles: their characteristic properties

and therapeutic applications. Nanoscale Research Letters 11(1):40.

Costa C, Conte A, Buonocore G, Lavorgna M, Del Nobile M. 2012. Calcium-alginate coating loaded with silver-montmorillonite nanoparticles to prolong the shelf-life of fresh-cut carrots. Food Research International 48(1):164-9.

Cruz-Romero M, Murphy T, Morris M, Cummins E, Kerry J. 2013. Antimicrobial activity of chitosan, organic acids and nano-sized solubilisates for potential use in smart antimicrobially-active packaging for potential food applications. Food Control 34(2):393-7.

Cui Y, Zhao Y, Tian Y, Zhang W, Lü X, Jiang X. 2012. The molecular mechanism of action of bactericidal gold nanoparticles on *Escherichia coli*. Biomaterials 33(7):2327-33.

Czaja W, Krystynowicz A, Kawecki M, Wysota K, Sakiel S, Wróblewski P, Glik J, Nowak M, Bielecki S. 2007. Biomedical applications of microbial cellulose in burn wound recovery. Cellulose: Molecular and Structural Biology: Springer. p. 307-21.

Davis M, Gordon D, Tarr P, Bartleson C, Lewis J, Barrett T, Wells J, Baron R, Kobayashi J. 1994. A multistate outbreak of *Escherichia coli* O157: H7—associated bloody diarrhea and hemolytic uremic syndrome from hamburgers: the washington experience. JAMA 272(17):1349-53.

DeMerlis C, Schoneker D. 2003. Review of the oral toxicity of polyvinyl alcohol (PVA). Food and Chemical Toxicology 41(3):319-26.

Deplanche K, Macaskie L. 2008. Biorecovery of gold by *Escherichia coli* and *Desulfovibrio desulfuricans*. Biotechnology and Bioengineering 99(5):1055-64.

Devasagayam T, Tilak J, Boloor K, Sane KS, Ghaskadbi SS, Lele R. 2004. Free radicals and antioxidants in human health: current status and future prospects. Japi 52(794804):4.

Du H, Hu Q, Yang W, Pei F, Kimatu BM, Ma N, Fang Y, Cao C, Zhao L. 2016. Development, physiochemical characterization and forming mechanism of *Flammulina velutipes* polysaccharide-based edible films. Carbohydrate Polymers 152:214-21.

Emam HE, Mowafi S, Mashaly HM, Rehan M. 2014. Production of antibacterial colored viscose fibers using in situ prepared spherical Ag nanoparticles. Carbohydrate Polymers 110:148-55.

Fahmy A, Kamoun EA, El-Eisawy R, El-Fakharany EM, Taha TH, El-Damhougy BK, Abdelhai F. 2015. Poly (vinyl alcohol)-hyaluronic acid membranes for wound dressing applications: synthesis and in vitro bio-evaluations. Journal of the Brazilian Chemical Society 26(7):1466-74.

Fathi E, Atyabi N, Imani M, Alinejad Z. 2011. Physically crosslinked polyvinyl alcohol–dextran blend xerogels: morphology and thermal behavior. Carbohydrate Polymers 84(1):145-52.

Feldman D. 1989. Polymeric building materials.

Feng QL, Wu J, Chen G, Cui F, Kim T, Kim J. 2000. A mechanistic study of the antibacterial effect of silver ions on *Escherichia coli* and *Staphylococcus*

aureus. Journal of Biomedical Materials Research 52(4):662-8.

Ferrer A, Pal L, Hubbe M. 2017. Nanocellulose in packaging: Advances in barrier layer technologies. Industrial Crops and Products 95:574-82.

Güçbilmez ÇM, Yemenicioğlu A, Arslanoğlu A. 2007. Antimicrobial and antioxidant activity of edible zein films incorporated with lysozyme, albumin proteins and disodium EDTA. Food Research International 40(1):80-91.

Gamage GR, Park H-J, Kim KM. 2009. Effectiveness of antimicrobial coated oriented polypropylene/polyethylene films in sprout packaging. Food Research International 42(7):832-9.

Gao X, Shi Z, Kuśmierczyk P, Liu C, Yang G, Sevostianov I, Silberschmidt VV. 2016. Time-dependent rheological behaviour of bacterial cellulose hydrogel. Materials Science and Engineering: C 58:153-9.

Gaume J, Wong-Wah-Chung P, Rivaton A, Thérias S, Gardette J-L. 2011. Photochemical behavior of PVA as an oxygen-barrier polymer for solar cell encapsulation. RSC Advances 1(8):1471-81.

George J, Sabapathi S. 2015. Cellulose nanocrystals: synthesis, functional properties, and applications. Nanotechnology, Science and Applications 8:45.

George S, Lin S, Ji Z, Thomas CR, Li L, Mecklenburg M, Meng H, Wang X, Zhang H, Xia T. 2012. Surface defects on plate-shaped silver nanoparticles contribute to its hazard potential in a fish gill cell line and zebrafish embryos. ACS Nano 6(5):3745-59.

González-Guisasola C, Ribes-Greus A. 2018. Dielectric relaxations and conductivity of cross-linked PVA/SSA/GO composite membranes for fuel cells. Polymer Testing 67:55-67.

Grande CJ, Torres FG, Gomez CM, Bañó MC. 2009. Nanocomposites of bacterial cellulose/hydroxyapatite for biomedical applications. Acta Biomaterialia 5(5):1605-15.

Greiling W. 1954. Paul Ehrlich. Düsseldorf: Econ Verlag:48.

Guhados G, Wan W, Hutter JL. 2005. Measurement of the elastic modulus of single bacterial cellulose fibers using atomic force microscopy. Langmuir 21(14):6642-6.

Guo D, Zhu L, Huang Z, Zhou H, Ge Y, Ma W, Wu J, Zhang X, Zhou X, Zhang Y. 2013. Anti-leukemia activity of PVP-coated silver nanoparticles via generation of reactive oxygen species and release of silver ions. Biomaterials 34(32):7884-94.

Guo Z, Zhang D, Wei S, Wang Z, Karki AB, Li Y, Bernazzani P, Young DP, Gomes J, Cocke DL. 2010. Effects of iron oxide nanoparticles on polyvinyl alcohol: interfacial layer and bulk nanocomposites thin film. Journal of Nanoparticle Research 12(7):2415-26.

Gurunathan S, Han JW, Eppakayala V, Jeyaraj M, Kim J-H. 2013. Cytotoxicity of biologically synthesized silver nanoparticles in MDA-MB-231 human breast cancer cells. BioMed Research International 2013.

Ha JH, Shah N, Ul-Islam M, Khan T, Park JK. 2011. Bacterial cellulose production from a single sugar α-linked glucuronic acid-based oligosaccharide. Process

Biochemistry 46(9):1717-23.
Hago E-E, Li X. 2013. Interpenetrating polymer network hydrogels based on gelatin and PVA by biocompatible approaches: synthesis and characterization. Advances in Materials Science and Engineering 2013.
Hamouda T, Baker J. 2000. Antimicrobial mechanism of action of surfactant lipid preparations in enteric Gram‐negative bacilli. Journal of Applied Microbiology 89(3):397-403.
Hampton MB, Orrenius S. 1997. Dual regulation of caspase activity by hydrogen peroxide: implications for apoptosis. FEBS Letters 414(3):552-6.
Han J, Castell-Perez M, Moreira R. 2007. The influence of electron beam irradiation of antimicrobial-coated LDPE/polyamide films on antimicrobial activity and film properties. LWT-Food Science and Technology 40(9):1545-54.
HÄNSCH K, KINKEL K. 1995. EUROPEAN PARLIAMENT AND COUNCIL DIRECTIVE 94/62/EC of 20 December 1994 on packaging and packaging waste. Journal of Environmental Law 7(2):323-37.
Hassan CM, Peppas NA. 2000. Structure and Applications of Poly(vinyl alcohol) Hydrogels Produced by Conventional Crosslinking or by Freezing/Thawing Methods. Biopolymers · PVA Hydrogels, Anionic Polymerisation Nanocomposites. Berlin, Heidelberg: Springer Berlin Heidelberg. p. 37-65.
Hawkins MJ, Soon-Shiong P, Desai N. 2008. Protein nanoparticles as drug carriers in clinical medicine. Advanced Drug Delivery Reviews 60(8):876-85.
He H, Cai R, Wang Y, Tao G, Guo P, Zuo H, Chen L, Liu X, Zhao P, Xia Q. 2017. Preparation and characterization of silk sericin/pva blend film with silver nanoparticles for potential antimicrobial application. International Journal of Biological Macromolecules 104:457-64.
He J, Kunitake T, Nakao A. 2003. Facile in situ synthesis of noble metal nanoparticles in porous cellulose fibers. Chemistry of Materials 15(23):4401-6.
Heinlaan M, Ivask A, Blinova I, Dubourguier H-C, Kahru A. 2008. Toxicity of nanosized and bulk ZnO, CuO and TiO2 to bacteria Vibrio fischeri and crustaceans Daphnia magna and Thamnocephalus platyurus. Chemosphere 71(7):1308-16.
Hestrin S, Schramm M. 1954. Synthesis of cellulose by Acetobacter xylinum. 2. Preparation of freeze-dried cells capable of polymerizing glucose to cellulose. Biochemical Journal 58(2):345.
Heydari R, Rashidipour M. 2015. Green synthesis of silver nanoparticles using extract of oak fruit hull (Jaft): synthesis and in vitro cytotoxic effect on MCF-7 cells. International Journal of Breast Cancer 2015.
Huang M-H, Yang M-C. 2008. Evaluation of glucan/poly (vinyl alcohol) blend wound dressing using rat models. International Journal of Pharmaceutics 346(1-2):38-46.
Huang Y, Li X, Liao Z, Zhang G, Liu Q, Tang J, Peng Y, Liu X, Luo Q. 2007. A randomized comparative trial between Acticoat and SD-Ag in the treatment of residual burn wounds, including safety analysis. Burns 33(2):161-6.
Hyon S-H, Cha W-I, Ikada Y. 1989. Preparation of transparent poly (vinyl alcohol)

hydrogel. Polymer Bulletin 22(2):119-22.
Jia Y, Zhai X, Fu W, Liu Y, Li F, Zhong C. 2016. Surfactant-free emulsions stabilized by tempo-oxidized bacterial cellulose. Carbohydrate Polymers 151:907-15.
Jin G, Zhang J, Yu X, Zhang Y, Lei Y, Wang J. 2010. Lipolysis and lipid oxidation in bacon during curing and drying–ripening. Food Chemistry 123(2):465-71.
Jin T, Sun D, Su J, Zhang H, Sue HJ. 2009. Antimicrobial efficacy of zinc oxide quantum dots against *Listeria monocytogenes*, *Salmonella enteritidis*, and *Escherichia coli* O157: H7. Journal of Food Science 74(1).
Joerger RD, Sabesan S, Visioli D, Urian D, Joerger MC. 2009. Antimicrobial activity of chitosan attached to ethylene copolymer films. Packaging Technology and Science 22(3):125-38.
Jones TF, Yackley J. 2018. Foodborne Disease Outbreaks in the United States: A Historical Overview. Foodborne Pathogens and Disease 15(1):11-5.
Jozala AF, de Lencastre-Novaes LC, Lopes AM, de Carvalho Santos-Ebinuma V, Mazzola PG, Pessoa-Jr A, Grotto D, Gerenutti M, Chaud MV. 2016. Bacterial nanocellulose production and application: a 10-year overview. Applied Microbiology and Biotechnology 100(5):2063-72.
Kalin M, Kuru S, Kismet K, Barlas AM, Akgun YA, Astarci HM, Ustun H, Ertas E. 2015. The effectiveness of porcine dermal collagen (Permacol®) on wound healing in the rat model. Indian Journal of Surgery 77(2):407-11.
Kamoun EA, Kenawy E-RS, Chen X. 2017. A review on polymeric hydrogel membranes for wound dressing applications: PVA-based hydrogel dressings. Journal of Advanced Research 8(3):217-33.
Kanmani P, Rhim J-W. 2014. Physicochemical properties of gelatin/silver nanoparticle antimicrobial composite films. Food Chemistry 148:162-9.
Kathiravan V, Ravi S, Ashokkumar S, Velmurugan S, Elumalai K, Khatiwada CP. 2015. Green synthesis of silver nanoparticles using Croton sparsiflorus morong leaf extract and their antibacterial and antifungal activities. Spectrochimica Acta Part A: Molecular and Biomolecular Spectroscopy 139:200-5.
Kelly K, Havrilla CM, Brady TC, Abramo KH, Levin ED. 1998. Oxidative stress in toxicology: established mammalian and emerging piscine model systems. Environmental Health Perspectives 106(7):375.
Khalil MM, Ismail EH, El-Baghdady KZ, Mohamed D. 2014. Green synthesis of silver nanoparticles using olive leaf extract and its antibacterial activity. Arabian Journal of Chemistry 7(6):1131-9.
Khaydarov RA, Khaydarov RR, Gapurova O, Estrin Y, Scheper T. 2009. Electrochemical method for the synthesis of silver nanoparticles. Journal of Nanoparticle Research 11(5):1193-200.
Kim J-H, Robertson RE, Naaman AE. 1999. Structure and properties of poly (vinyl alcohol)-modified mortar and concrete1. Cement and Concrete Research 29(3):407-15.
Kreuter J. 2007. Nanoparticles—a historical perspective. International Journal of Pharmaceutics 331(1):1-10.

Laux P, Tentschert J, Riebeling C, Braeuning A, Creutzenberg O, Epp A, Fessard V, Haas K-H, Haase A, Hund-Rinke K. 2017. Nanomaterials: certain aspects of application, risk assessment and risk communication. Archives of Toxicology:1-21.

Levard C, Hotze EM, Colman BP, Dale AL, Truong L, Yang X, Bone AJ, Brown Jr GE, Tanguay RL, Di Giulio RT. 2013. Sulfidation of silver nanoparticles: natural antidote to their toxicity. Environmental Science & Technology 47(23):13440-8.

Li Z, Wang L, Chen S, Feng C, Chen S, Yin N, Yang J, Wang H, Xu Y. 2015. Facilely green synthesis of silver nanoparticles into bacterial cellulose. Cellulose 22(1):373-83.

Lim M, Kim D, Seo J, Han H. 2014. Preparation and properties of poly (vinyl alcohol)/vinyltrimethoxysilane (PVA/VTMS) hybrid films with enhanced thermal stability and oxygen barrier properties. Macromolecular Research 22(10):1096-103.

Lin C-C, Lee L-T, Hsu L-J. 2014. Degradation of polyvinyl alcohol in aqueous solutions using UV-365 nm/S 2 O 8 2− process. International Journal of Environmental Science and Technology 11(3):831-8.

Lin K, Lin H. 2004. Quality Characteristics of Chinese‐style Meatball Containing Bacterial Cellulose (Nata). Journal of Food Science 69(3).

Liu H, Lian T, Liu Y, Hong Y, Sun D, Li Q. 2017. Plant-mediated synthesis of Au nanoparticles: Separation and identification of active biomolecule in the water extract of Cacumen Platycladi. Industrial & Engineering Chemistry Research 56(18):5262-70.

Liu J, Detrembleur C, Pauw‐Gillet D, Mornet S, Jérôme C, Duguet E. 2015. Gold Nanorods Coated with Mesoporous Silica Shell as Drug Delivery System for Remote Near Infrared Light‐Activated Release and Potential Phototherapy. Small 11(19):2323-32.

Liz-Marzán LM. 2004. Nanometals: formation and color. Materials Today 7(2):26-31.

Lojk J, Bregar VB, Strojan K, Hudoklin S, Veranič P, Pavlin M, Kreft ME. 2018. Increased endocytosis of magnetic nanoparticles into cancerous urothelial cells versus normal urothelial cells. Histochemistry and Cell Biology 149(1):45-59.

Love AJ, Makarov VV, Sinitsyna OV, Shaw J, Yaminsky IV, Kalinina NO, Taliansky M. 2015. A genetically modified tobacco mosaic virus that can produce gold nanoparticles from a metal salt precursor. Frontiers in Plant Science 6:984.

Lu X, Dong X, Zhang K, Han X, Fang X, Zhang Y. 2013. A gold nanorods-based fluorescent biosensor for the detection of hepatitis B virus DNA based on fluorescence resonance energy transfer. Analyst 138(2):642-50.

Mandal D, Dash SK, Das B, Chattopadhyay S, Ghosh T, Das D, Roy S. 2016. Bio-fabricated silver nanoparticles preferentially targets Gram positive depending on cell surface charge. Biomedicine & Pharmacotherapy 83:548-58.

Maneerung T, Tokura S, Rujiravanit R. 2008. Impregnation of silver nanoparticles into bacterial cellulose for antimicrobial wound dressing. Carbohydrate

Polymers 72(1):43-51.
Mannan M, Alexander J, Ganapathy C, Teo D. 2006. Quality improvement of oil palm shell (OPS) as coarse aggregate in lightweight concrete. Building and Environment 41(9):1239-42.
Marchiore NG, Manso IJ, Kaufmann KC, Lemes GF, de Oliveira Pizolli AP, Droval AA, Bracht L, Goncalves OH, Leimann FV. 2017. Migration evaluation of silver nanoparticles from antimicrobial edible coating to sausages. LWT-Food Science and Technology 76:203-8.
Marder EP, Griffin PM, Cieslak PR, Dunn J, Hurd S, Jervis R, Lathrop S, Muse A, Ryan P, Smith K. 2018. Preliminary Incidence and Trends of Infections with Pathogens Transmitted Commonly Through Food—Foodborne Diseases Active Surveillance Network, 10 US Sites, 2006–2017. Morbidity and Mortality Weekly Report 67(11):324.
Maria TM, De Carvalho RA, Sobral PJ, Habitante AMB, Solorza-Feria J. 2008. The effect of the degree of hydrolysis of the PVA and the plasticizer concentration on the color, opacity, and thermal and mechanical properties of films based on PVA and gelatin blends. Journal of Food Engineering 87(2):191-9.
McQuillan JS, Groenaga Infante H, Stokes E, Shaw AM. 2012. Silver nanoparticle enhanced silver ion stress response in *Escherichia coli* K12. Nanotoxicology 6(8):857-66.
Miller G, Senjen R. 2008. Out of the Laboratory and onto our Plates: Nanotechnology in Food & Agriculture. A report prepared for Friends of the Earth Australia. Friends of the Earth Europe and Friends of the Earth United States and supported by Friends of the Earth Germany Friends of the Earth Australia Nanotechnology Project, Australia.
Mironava T, Simon M, Rafailovich MH, Rigas B. 2013. Platinum folate nanoparticles toxicity: cancer vs. normal cells. Toxicology in Vitro 27(2):882-9.
Mukherjee P, Ahmad A, Mandal D, Senapati S, Sainkar SR, Khan MI, Parishcha R, Ajaykumar P, Alam M, Kumar R. 2001. Fungus-mediated synthesis of silver nanoparticles and their immobilization in the mycelial matrix: a novel biological approach to nanoparticle synthesis. Nano Letters 1(10):515-9.
Mulfinger L, Solomon SD, Bahadory M, Jeyarajasingam AV, Rutkowsky SA, Boritz C. 2007. Synthesis and study of silver nanoparticles. Journal of Chemical Education 84(2):322.
Muriel-Galet V, Cerisuelo JP, López-Carballo G, Lara M, Gavara R, Hernández-Muñoz P. 2012. Development of antimicrobial films for microbiological control of packaged salad. International Journal of Food Microbiology 157(2):195-201.
Muthuvel A, Adavallan K, Balamurugan K, Krishnakumar N. 2014. Biosynthesis of gold nanoparticles using Solanum nigrum leaf extract and screening their free radical scavenging and antibacterial properties. Biomedicine & Preventive Nutrition 4(2):325-32.
Nadarajah D, Han J, Holley R. 2005. Inactivation of *Escherichia coli* O157: H7 in packaged ground beef by allyl isothiocyanate. International Journal of Food

Microbiology 99(3):269-79.
Nahar M, Dutta T, Murugesan S, Asthana A, Mishra D, Rajkumar V, Tare M, Saraf S, Jain NK. 2006. Functional polymeric nanoparticles: an efficient and promising tool for active delivery of bioactives. Critical Reviews™ in Therapeutic Drug Carrier Systems 23(4).
Nam SY, Nho YC, Hong SH, Chae GT, Jang HS, Suh TS, Ahn WS, Ryu KE, Chun HJ. 2004. Evaluations of poly (vinyl alcohol)/alginate hydrogels cross-linked by γ-ray irradiation technique. Macromolecular Research 12(2):219-24.
Ng T, Ching Y, Awanis N, Ishenny N, Rahman M. 2014. Effect of bleaching condition on thermal properties and UV transmittance of PVA/cellulose biocomposites. Materials Research Innovations 18(sup6):S6-400-S6-4.
Ougiya H, Watanabe K, Morinaga Y, Yoshinaga F. 1997. Emulsion-stabilizing effect of bacterial cellulose. Bioscience, Biotechnology, and Biochemistry 61(9):1541-5.
Owen RW, Giacosa A, Hull WE, Haubner R, Würtele G, Spiegelhalder B, Bartsch H. 2000. Olive-oil consumption and health: the possible role of antioxidants. The Lancet Oncology 1(2):107-12.
Pandit R, Rai M, Santos CA. 2017. Enhanced antimicrobial activity of the food-protecting nisin peptide by bioconjugation with silver nanoparticles. Environmental Chemistry Letters 15(3):443-52.
Paschoalick T, Garcia F, Sobral PdA, Habitante A. 2003. Characterization of some functional properties of edible films based on muscle proteins of Nile Tilapia. Food Hydrocolloids 17(4):419-27.
Pelgrift RY, Friedman AJ. 2013. Nanotechnology as a therapeutic tool to combat microbial resistance. Advanced Drug Delivery Reviews 65(13-14):1803-15.
Peng J-m, Lin J-c, Chen Z-y, Wei M-c, Fu Y-x, Lu S-s, Yu D-s, Zhao W. 2017. Enhanced antimicrobial activities of silver-nanoparticle-decorated reduced graphene nanocomposites against oral pathogens. Materials Science and Engineering: C 71:10-6.
Pereira AG, Muniz EC, Hsieh Y-L. 2014. Chitosan-sheath and chitin-core nanowhiskers. Carbohydrate Polymers 107:158-66.
Pereira Jr VA, de Arruda INQ, Stefani R. 2015. Active chitosan/PVA films with anthocyanins from Brassica oleraceae (Red Cabbage) as Time–Temperature Indicators for application in intelligent food packaging. Food Hydrocolloids 43:180-8.
Pramanik A, Laha D, Bhattacharya D, Pramanik P, Karmakar P. 2012. A novel study of antibacterial activity of copper iodide nanoparticle mediated by DNA and membrane damage. Colloids and Surfaces B: Biointerfaces 96:50-5.
Rajwade J, Paknikar K, Kumbhar J. 2015. Applications of bacterial cellulose and its composites in biomedicine. Applied Microbiology and Biotechnology 99(6):2491-511.
Ramos M, Jiménez A, Peltzer M, Garrigós MC. 2012. Characterization and antimicrobial activity studies of polypropylene films with carvacrol and thymol for active packaging. Journal of Food Engineering 109(3):513-9.

Raveendran P, Fu J, Wallen SL. 2003. Completely “green” synthesis and stabilization of metal nanoparticles. Journal of the American Chemical Society 125(46):13940-1.

Rehan M, Barhoum A, Van Assche G, Dufresne A, Gätjen L, Wilken R. 2017. Towards multifunctional cellulosic fabric: UV photo-reduction and in-situ synthesis of silver nanoparticles into cellulose fabrics. International Journal of Biological Macromolecules 98:877-86.

Reidy B, Haase A, Luch A, Dawson KA, Lynch I. 2013. Mechanisms of silver nanoparticle release, transformation and toxicity: a critical review of current knowledge and recommendations for future studies and applications. Materials 6(6):2295-350.

Rhim J, Wang L, Hong S. 2013. Preparation and characterization of agar/silver nanoparticles composite films with antimicrobial activity. Food Hydrocolloids 33(2):327-35.

Ribeiro A, Anbu S, Alegria E, Fernandes A, Baptista P, Mendes R, Matias A, Mendes M, da Silva MG, Pombeiro A. 2018. Evaluation of cell toxicity and DNA and protein binding of green synthesized silver nanoparticles. Biomedicine & Pharmacotherapy 101:137-44.

Ro EY, Ko YM, Yoon KS. 2015. Survival of pathogenic enterohemorrhagic *Escherichia coli* (EHEC) and control with calcium oxide in frozen meat products. Food Microbiology 49:203-10.

Samberg ME, Oldenburg SJ, Monteiro-Riviere NA. 2010. Evaluation of silver nanoparticle toxicity in skin in vivo and keratinocytes in vitro. Environmental Health Perspectives 118(3):407.

Sarwar MS, Niazi MBK, Jahan Z, Ahmad T, Hussain A. 2018. Preparation and characterization of PVA/nanocellulose/Ag nanocomposite films for antimicrobial food packaging. Carbohydrate Polymers.

Seong M, Lee DG. 2017. Silver Nanoparticles Against *Salmonella enterica Serotype Typhimurium*: Role of Inner Membrane Dysfunction. Current Microbiology 74(6):661-70.

Shah N, Ul-Islam M, Khattak WA, Park JK. 2013. Overview of bacterial cellulose composites: a multipurpose advanced material. Carbohydrate Polymers 98(2):1585-98.

Shi Z, Zhang Y, Phillips GO, Yang G. 2014. Utilization of bacterial cellulose in food. Food Hydrocolloids 35:539-45.

Shishkova I, Yastrebov A. 2015. Evaporation and condensation in the presence of nanoparticles in bulk vapor. Colloid Journal 77(5):661-7.

Shoda M, Sugano Y. 2005. Recent advances in bacterial cellulose production. Biotechnology and Bioprocess Engineering 10(1):1.

Shukla R, Bansal V, Chaudhary M, Basu A, Bhonde RR, Sastry M. 2005. Biocompatibility of gold nanoparticles and their endocytotic fate inside the cellular compartment: a microscopic overview. Langmuir 21(23):10644-54.

Solano ACV, de Rojas Gante C. 2012. Two different processes to obtain antimicrobial packaging containing natural oils. Food and Bioprocess Technology

5(6):2522-8.
Sondi I, Salopek-Sondi B. 2004. Silver nanoparticles as antimicrobial agent: a case study on *E. coli* as a model for Gram-negative bacteria. Journal of Colloid and Interface Science 275(1):177-82.
Sood A, Granick MS, Tomaselli NL. 2014. Wound dressings and comparative effectiveness data. Advances in Wound Care 3(8):511-29.
Sotiriou GA, Sannomiya T, Teleki A, Krumeich F, Vörös J, Pratsinis SE. 2010. Non‐toxic dry‐coated nanosilver for plasmonic biosensors. Advanced Functional Materials 20(24):4250-7.
Spaic M, Small DP, Cook JR, Wan W. 2014. Characterization of anionic and cationic functionalized bacterial cellulose nanofibres for controlled release applications. Cellulose 21(3):1529-40.
Spence KL, Venditti RA, Rojas OJ, Pawlak JJ, Hubbe MA. 2011. Water vapor barrier properties of coated and filled microfibrillated cellulose composite films. BioResources 6(4):4370-88.
Stamplecoskie KG, Scaiano JC, Tiwari VS, Anis H. 2011. Optimal size of silver nanoparticles for surface-enhanced Raman spectroscopy. The Journal of Physical Chemistry C 115(5):1403-9.
Sukirtha R, Priyanka KM, Antony JJ, Kamalakkannan S, Thangam R, Gunasekaran P, Krishnan M, Achiraman S. 2012. Cytotoxic effect of Green synthesized silver nanoparticles using Melia azedarach against in vitro HeLa cell lines and lymphoma mice model. Process Biochemistry 47(2):273-9.
Sulaeva I, Henniges U, Rosenau T, Potthast A. 2015. Bacterial cellulose as a material for wound treatment: Properties and modifications. A review. Biotechnology Advances 33(8):1547-71.
Sung S-Y, Sin LT, Tee T-T, Bee S-T, Rahmat A, Rahman W, Tan A-C, Vikhraman M. 2013. Antimicrobial agents for food packaging applications. Trends in Food Science & Technology 33(2):110-23.
Suppakul P, Miltz J, Sonneveld K, Bigger SW. 2002. Preliminary study of antimicrobial films containing the principal constituents of basil. World Conference on Packaging: Proceedings of the 13th Intl. Assoc. of Packaging Res. Inst., Michigan State Univ., East Lansing, Mich., June. p. 23-8.
Tang J, Bao L, Li X, Chen L, Hong FF. 2015. Potential of PVA-doped bacterial nano-cellulose tubular composites for artificial blood vessels. Journal of Materials Chemistry B 3(43):8537-47.
Tao G, Liu L, Wang Y, Chang H, Zhao P, Zuo H, He H. 2016. Characterization of silver nanoparticle in situ synthesis on porous sericin gel for antibacterial application. Journal of Nanomaterials 2016.
Thong C, Teo D, Ng C. 2016. Application of polyvinyl alcohol (PVA) in cement-based composite materials: A review of its engineering properties and microstructure behavior. Construction and Building Materials 107:172-80.
Tian X, Jiang X, Welch C, Croley TR, Wong T-Y, Chen C, Fan S, Chong Y, Li R, Ge C. 2018. Bactericidal Effects of Silver Nanoparticles on *Lactobacilli* and the Underlying Mechanism. ACS Applied Materials & Interfaces 10(10):8443-50.

Tripathi S, Mehrotra G, Dutta P. 2009. Physicochemical and bioactivity of cross-linked chitosan–PVA film for food packaging applications. International Journal of Biological Macromolecules 45(4):372-6.

Turner S, Kumar M. 2018. Cellulose synthase complex organization and cellulose microfibril structure. Phil. Trans. R. Soc. A 376(2112):20170048.

Ullah H, Santos HA, Khan T. 2016. Applications of bacterial cellulose in food, cosmetics and drug delivery. Cellulose 23(4):2291-314.

Veeraputhiran V. 2013. Bio-catalytic synthesis of silver nanoparticles. Int J Chem Tech Res 5(5):255-2562.

Wan Y, Zhang D, Wang Y, Qi P, Wu J, Hou B. 2011. Vancomycin-functionalised Ag@ TiO2 phototoxicity for bacteria. Journal of Hazardous Materials 186(1):306-12.

Wang S, Lawson R, Ray PC, Yu H. 2011. Toxic effects of gold nanoparticles on *Salmonella typhimurium* bacteria. Toxicology and Industrial Health 27(6):547-54.

Wang W, Alexandridis P. 2016. Composite polymer electrolytes: Nanoparticles affect structure and properties. Polymers 8(11):387.

Wu R, Qu J, He H, Yu Y. 2004. Removal of azo-dye Acid Red B (ARB) by adsorption and catalytic combustion using magnetic CuFe2O4 powder. Applied Catalysis B: Environmental 48(1):49-56.

Yamanaka S, Watanabe K, Kitamura N, Iguchi M, Mitsuhashi S, Nishi Y, Uryu M. 1989. The structure and mechanical properties of sheets prepared from bacterial cellulose. Journal of Materials Science 24(9):3141-5.

Yang G, Xie J, Deng Y, Bian Y, Hong F. 2012a. Hydrothermal synthesis of bacterial cellulose/AgNPs composite: a "green" route for antibacterial application. Carbohydrate Polymers 87(4):2482-7.

Yang G, Xie J, Hong F, Cao Z, Yang X. 2012b. Antimicrobial activity of silver nanoparticle impregnated bacterial cellulose membrane: effect of fermentation carbon sources of bacterial cellulose. Carbohydrate Polymers 87(1):839-45.

Yang JM, Su WY, Yang MC. 2004. Evaluation of chitosan/PVA blended hydrogel membranes. journal of Membrane Science 236(1-2):39-51.

Yu SY, Lin KW. 2014. Influence of Bacterial Cellulose (nata) on the Physicochemical and Sensory Properties of Frankfurter. Journal of Food Science 79(6).

Zhang G, Qu J, Liu H, Liu R, Wu R. 2007. Preparation and evaluation of a novel Fe–Mn binary oxide adsorbent for effective arsenite removal. Water Research 41(9):1921-8.

Zhang X-F, Liu Z-G, Shen W, Gurunathan S. 2016. Silver nanoparticles: synthesis, characterization, properties, applications, and therapeutic approaches. International Journal of Molecular Sciences 17(9):1534.

Zhang X, He X, Wang K, Wang Y, Li H, Tan W. 2009. Biosynthesis of size-controlled gold nanoparticles using fungus, Penicillium sp. Journal of Nanoscience and Nanotechnology 9(10):5738-44.

Zhao L, Mitomo H, Zhai M, Yoshii F, Nagasawa N, Kume T. 2003. Synthesis of antibacterial PVA/CM-chitosan blend hydrogels with electron beam irradiation.

Carbohydrate Polymers 53(4):439-46.
Zhao X, Hilliard LR, Mechery SJ, Wang Y, Bagwe RP, Jin S, Tan W. 2004. A rapid bioassay for single bacterial cell quantitation using bioconjugated nanoparticles. Proceedings of the National Academy of Sciences of the United States of America 101(42):15027-32.